TECHNISCHE UNIVERSITÄT MÜNCHEN

Fakultät für Medizin

# Detection of DNA-Alterations Caused by Sulfur Mustard and its Derivatives via Immunoslotblot

Verena Justine Schrettl

Vollständiger Abdruck der von der Fakultät für Medizin der Technischen Universität München zur Erlangung des akademischen Grades einer

Doktorin der Medizin

genehmigten Dissertation.

| | |
|---|---|
| Vorsitzender: | Prof. Dr. Ernst J Rummeny |
| Prüfer der Dissertation: | 1. apl. Prof. Dr. Horst Thiermann |
| | 2. Prof. Dr. Florian Eyer |

Die Dissertation wurde am 08.07.2022 bei der Technischen Universität München eingereicht und durch die Fakultät für Medizin am 08.11.2022 angenommen.

*To my great, loud, and loving family! Love you guys!*

# Acknowledgments

I would like to thank everyone who has been a part of this work and who helped me along the way. Special thanks go to my doctoral adviser Prof. Dr. Horst Thiermann and to my supervisor Prof. Dr. Kai Kehe. Without their help and continued support it would not have been possible for me to carry out the work and finish my thesis. Additionally, I would like to thank Stefan Müller, Rham Prassad, and Mina Zarrabi all of whom supported me throughout my laboratory work and patiently answered all my questions.

Finally, I would like to thank my parents and my siblings. Without your moral support this process would have been much more difficult! Thank you very much!

## Summary

The chemical warfare agent sulfur mustard (bis(2-chloroethyl) sulfide) and its different derivatives are classified as vesicant agents. If exposed to the agent, humans may be incapacitated after a period of latency and suffer from severe damages to the eyes, the skin, the lung and other tissues. The agent causes alterations of the DNA, RNA and proteins, the so-called alkylation, which is assumed to be the underlying mechanism for most of the pathophysiological effects. Alterations of the DNA may be detected by immunological methods, e.g. the immunoslotblot technique using the primary monoclonal antibody 2F8. This antibody was developed to detect DNA adducts caused by sulfur mustard. The main goal of the present thesis is to use the immunoslotblot technique employing the primary monoclonal antibody 2F8 to detect DNA adducts caused by bis(2-chloroethyl) sulfide, 2-chloroethyl ethyl sulfide, and the three nitrogen mustards in order to evaluate the detection limit of this method. Furthermore, different dyeing agents such as 3,3`-diaminobenzidin, Seramun Grün®, and Seramun Blau® were investigated for their usefulness in these tests with the aim to develop a standard method with high sensitivity.

In this study, a statistically significant difference between the negative control and the exposed samples, indicated by $p < 0.05$, could be detected for 2-chloroethyl ethyl sulfide with the dyeing agents 3,3`-diaminobenzidin, Seramun Blau®, and Seramun Grün® down to concentrations of 30 µM, 3 µM, and 30 µM, respectively. For bis(2-chloroethyl) sulfide, DNA adducts were detectable with 3,3`-diaminobenzidin and Seramun Grün® down to concentration of 0.3 µM and 1 µM, respectively. Finally, no statistically significant difference between the negative control and the exposed DNA samples could be detected for the investigated nitrogen derivatives of bis(2-chloroethyl) sulfide.

Our investigations show that the immunoslotblot technique using the primary monoclonal antibody 2F8 allows detection of DNA alterations that are caused by the chemical warfare agents 2-chloroethyl ethyl sulfide and bis(2-chloroethyl) sulfide. Further experiments need to be performed to further develop the method for its clinical use and in order to ascertain whether such tests can detect exposure to the chemical warfare agents bis(2-chloroethyl) sulfide and 2-chloroethyl ethyl sulfide from DNA found in blister roofs. Similarly, for the detection of DNA alterations caused by the nitrogen mustard derivatives further investigation of the method is required.



## Keywords

Chemical Warfare Agents, Sulfur Mustard, Nitrogen Mustard, DNA Adducts, Immunoslotblot

## Zusammenfassung

Der chemische Kampfstoff Schwefel Lost (Bis(2-chloroethyl)sulfid) und seine verschiedenen Derivate werden als blasenbildende Stoffe klassifiziert. In Folge einer Exposition können bei Betroffenen nach einer Latenzphase Schädigungen der Augen, der Haut, der Lunge oder anderer Gewebe auftreten. Die Substanz verursacht Veränderungen der DNA, der RNA und von Proteinen. Es wird vermutet, dass diese so genannte Alkylierung für die pathophysiologischen Veränderungen verantwortlich ist. Die DNA-Veränderungen können durch immunologische Methoden wie dem Immunoslotblot mit Hilfe des primären monoklonalen Antikörpers 2F8 festgestellt werden. Der Antikörper wurde speziell dafür entwickelt, durch Schwefel Lost verursachte DNA-Addukte zu identifizieren. Das Hauptziel dieser Arbeit besteht darin, die Immunoslotblot-Technik mit dem primären monoklonalen Antiköper 2F8 zu verwenden, um DNA-Addukte, die durch Bis(2-chloroethyl)sulfid, 2-Chloroethyl-ethyl-sulfid und drei Stickstoff-Derivate verursacht werden, zu identifizieren. Das weitere Ziel ist, die Grenzen der Detektion nach der Einwirkung dieser Kampfstoffe zu bestimmen. Darüber hinaus wird die Sensitivität verschiedener Farbstoffe getestet, um die Basis für eine Standardmethode zum Nachweis von DNA-Addukten zu schaffen.

Ein statistisch signifikanter Unterschied zwischen der Negativkontrolle und den exponierten DNA Proben, mit $p < 0{,}05$, konnte für 2-Chloroethyl-ethyl-sulfid mit den Farbstoffen 3,3`-Diaminobenzidin, Seramun Blau® und Seramun Grün® bis zu einer Konzentration von 30 µM, 3 µM beziehungsweise 30 µM gefunden werden. Für Bis(2-chloroethyl)sulfid waren DNA Addukte mit den Farbstoffen 3,3`-Diaminobenzidin und Seramun Grün® bis zu einer Konzentration von 0.3 µM beziehungsweise 1 µM feststellbar. Im Gegensatz dazu konnte für die untersuchten Stickstoffderivate von Bis(2-chloroethyl)sulfid kein statistisch signifikanter Unterschied zwischen der Negativkontrolle und den exponierten DNA-Proben konstatiert werden.

Die durchgeführten Untersuchungen zeigen, dass die Immunoslotblot-Technik mit dem primären monoklonalen Antiköper 2F8 eingesetzt werden kann, um durch Exposition gegenüber den chemischen Kampfstoffen Bis(2-chloroethyl)sulfid und 2-Chloroethyl-ethyl-sulfid hervorgerufene DNA-Veränderungen nachzuweisen. Es bedarf weiterer Experimente, um diese Methode zur klinischen Anwendung weiter zu entwickeln und um damit auch DNA-Veränderungen aus dem Gewebe bereits gebildeter Hautblasen nachzuweisen. Um gleichzeitig auch DNA-Veränderungen, die durch die Stickstoffloste verursacht worden sind ebenso zu erkennen, bedarf es weiterer Experimente.

## Schlüsselwörter

Chemische Kampfstoffe, Senfgas, Stickstofflost, DNA-Addukte, Immunoslotblot

# Table of Contents

# List of Figures

# List of Tables

# List of Abbreviation

| | |
|---|---|
| ADP | adenosine diphosphate |
| AEGL | acute emergency guideline levels |
| ATM | ataxia teleangiectasia mutated protein |
| ATP | adenosine triphosphate |
| ATR | ataxia teleangiectasia and Rad3 related kinase |
| a.u. | arbitrary units |
| B.C. | before Christ |
| BArch | Bundesarchiv |
| BAL | bronchoalveolar lavage |
| Bcl-2 | B-cell lymphoma |
| bp | basis points |
| °C | degree Celsius |
| C | control |
| CAS | chemical abstracts service |
| CEES | 2-chlorethyl ethyl sulfide |
| $cm^2$ | square centimeter |
| $CO_2$ | carbon dioxide |
| CW | chemical warfare |
| CWA | chemical warfare agent |
| CWC | chemical weapons convention |
| DAB | 3,3'-diaminobenzidine |
| DMEM | Dulbecco´s modified Eagle medium |
| DNA | deoxyribonucleic acid |
| DR-4 | death receptor 4 |
| DR-5 | death receptor 5 |
| e.g. | exempli gratia |
| ESI MS | electrospray ionization mass-spectrometry |
| ESI-MS-MS | electrospray ionization tandem-mass-spectrometry |
| FADD | Fas-associated protein with death domain |
| FasL | Fas-ligand |
| FEV | forced vital capacity |
| FEV1 | forced vital capacity in one second |
| FKS | fetal calf serum |
| g | gram |
| *g* | gravitational force |
| G1 | checkpoint of the cell cycle |
| G2 | checkpoint of the cell cycle |
| GC-MS | gas chromatography–mass spectrometry |
| H | Hun Stuff |
| h | hour |
| HaCAT | human immortalized keratinocyte |
| HETE-CP | hydroxyethylthioethyl-cysteine-proline |
| HN-1 | bis(2-chloroethyl) ethylamine |
| HN-2 | bis(2-chloroethyl) methylamine |

| | |
|---|---|
| HN-3 | tris(2-chloroethyl) amine |
| HRP | horseradish peroxidase |
| IQR | interquartile range |
| ISIL | Islamic State of Iraq and Levant |
| kg | kilogram |
| L | liter |
| LC | liquid chromatography |
| LD50 | median lethal dose |
| M | mole |
| m | meter |
| mbar | millibar |
| MEM | modified Eagle's medium |
| µg | microgram |
| mg | milligram |
| min | minute |
| mL | milliliter |
| µM | micromolar |
| mM | millimolar |
| µm | micrometer |
| mm | millimeter |
| mmHg | millimeter of mercury |
| µmol | micromole |
| mmol | millimole |
| MOMP | mitochondrial outer membrane permeabilization |
| N7-HETE-dG | *N*7-hydroxyethylthioethyl-2´-deoxyguanosine |
| $NAD^+$ | nicotinamide adenine dinucleotide |
| NATO | North Atlantic Treaty Organization |
| ng | nanogram |
| nm | nanometer |
| nM | nanomolar |
| OPCW | organization for the prohibition of chemical weapons |
| p53 | regulator of the cell cycle |
| PARP | poly-ADP ribose polymerase |
| PARP-1 | poly-ADP ribose polymerase-1 |
| PBS | phosphate-buffered saline |
| pH | potentia hydrogenii |
| RNA | ribonucleic acid |
| RNase | ribonuclease |
| RSDL | reactive skin decontamination lotion |
| s | second |
| SM | sulfur mustard, (bis(2-chloroethyl) sulfide), S-Lost |
| SSC buffer | saline sodium citrate buffer |
| TGF-beta | transforming growth factor beta |
| TNF | tumor necrosis factor |
| UN | United Nations |
| US | United States |
| WBC | white blood cell count |

# 1

# Introduction

# 1 Introduction

## 1.1 Chemical Warfare Agents

Chemical warfare agents (CWAs) form a subgroup of the so-called weapons of mass destruction, as they are intended to affect a large group of people. Weapons of mass destruction are defined as: "nuclear, radiological, chemical, and/or biological weapons intended to produce mass casualties" [1–4]. The use of CWAs is banned by the chemical weapons convention (CWC), which is currently in force in 193 states (as of 22 September 2021) [5]. Article II of the CWC provides a definition of a chemical weapon:

"[The term] "Chemical Weapons" means the following, together or separately:

*a)* Toxic chemicals and their precursors, except where intended for purposes not prohibited under this Convention, as long as the types and quantities are consistent with such purposes;

*b)* Munitions and devices, specifically designed to cause death or other harm through the toxic properties of those toxic chemicals specified in subparagraph *(a)*, which would be released as a result of the employment of such munitions and devices;

*c)* Any equipment specifically designed for use directly in connection with the employment of munitions and devices specified in subparagraph *(b)*."

Anybody can be exposed to CWAs either by terrorist-, military- or homicidal-attacks, by inadvertently coming into contact with old stockpiles, or in industrial sites such as facilities used for the destruction of CWAs. Although CWAs are easy to obtain and to produce [4,6,7], disseminating them for military purposes is far more difficult, especially when it is intended to cause a large number of casualties or for military tactical purposes. One important feature of this aspect can best be explained by assessing the agents' chemical and physical characteristics, as will be elucidated for sulfur mustard (SM) in greater detail in Section 1.3 of the present thesis.

Beyond the setting of acute warfare or its aftermath, terrorist groups present an ongoing threat and CWAs have been used in the context of their attacks, as was the case in Tokyo in 1994 and 1995, where a terrorist group used the nerve agent sarin, in Syria during the civil war in 2013, where sarin and sulfur mustard was used, in Salisbury in 2018 and in Tomsk in 2020, where the nerve agent Novichok was used against Sergej and Yulia Skripal and Alexej Navalny, respectively. And in 2017 Kim Jon Nam was assassinated by exposing him to the nerve agent VX [8–14].

Unfortunately, manuals for easy synthesis of some CWAs are available on the internet, the requirements for the infrastructure are not high and many educts can be purchased. In addition, stocks of CWAs that have not been properly disposed of constitute a potential resource for terrorist groups, as exemplified by barrels of sulfur mustard from World War I that were dumped into the Baltic Sea as well as the Atlantic Ocean along the US east coast, where they were accidentally caught by fishermen [15]. The detection of CWAs in the environment and, even more so, detecting exposure to a CWA is therefore of utmost importance to be able to protect and perform countermeasures.

Armed forces and non-governmental organizations have been challenged with the decontamination and destruction of chemical warfare agents including sulfur mustard as the Chemical Warfare Convention came into force [16]. However, prior to destructing these substances, the involved organizations need to identify them first. In both settings, identifying unknown substances and destroying previously identified substances, one can get exposed to these substances. However, it is not always certain, whether actual exposure took place or not.

There exist various ways of detecting vaporized and liquid forms of CWAs in the environment [17]. For example, the analysis of air and liquids can be carried out with portable ion mobility spectrometers such as the so-called *chemical agent monitor* or other versions of this detector [18]. Moreover, vaporized agents can be detected with appropriate kits for CWAs such as the M256A1 chemical agent detector kit that features a set of chemical reagents that become colored upon reaction with air-borne agents [18]. Liquids can also be analyzed with paper indicator tests such as the M8 or M9 chemical detection paper that becomes colored if a reaction with a CWA occurs [18]. Sulfur and nitrogen vesicants, which are the focus of this thesis can be detected by further special kits either in vaporized or in liquid form [19].

However, in scenarios without pre-warning systems for immediate detection, environmental samples will not be analyzed within a short period of time and the health care system will have to deal with patients without knowing the cause of poisoning. The onset of the first symptoms may take anything from a few minutes (volatile nerve agents) to a couple of hours (sulfur mustard, phosgene), depending on the specific type of CWA and there will be the need for a clinical diagnosis, fast decontamination and start of treatment. In such cases, biomedical sampling to identify the poison should be postponed to a time after this procedure. Therefore, however, the clinical diagnosis must be made as fast as possible. This thesis focuses on the investigation on how such an identification can be accomplished for sulfur mustard and its derivatives in the early phase of poisoning.

A serious threat to use or even actual use of CWAs can trigger substantial psychological and physical stress to the population. In a setting with potential CWA attacks the uncertainty as to

whether one had contact to a CWA can cause panic among civilians and military personnel, as well as trigger somatic reactions, especially after missile attacks, as was seen in Israel during the Gulf War, in Tokyo in 1995 during the terrorist sarin attacks and recently in Syria, Salisbury, Omsk and Malaysia [1,4,6,7,9–12]. In addition to the medical effects and healthcare efforts in the aftermath of a CWA incident, there are considerable economic and financial consequences to consider. This includes the efforts for the protection and evacuation of the population, and the costs of detecting and decontaminating the affected areas, which can be substantial [20]. Chemical warfare agents can be and was a threat to uninvolved civilians as could be seen in the Novichok attack in Salisbury, where two uninvolved were affected (one died, one has gone blind) [21] or in the case of Nawalny [9].

In conclusion, warfare agents can affect governmental (army, police and fire department) and non-governmental organizations (civilians, public social aid), industry as well as general population and may force to take protective measures (e.g. collective protection) or use of masks up to permanently wear special protective gears [19,20].

First, a brief overview of the history of the use of sulfur mustard as a CWA will be given (Section 1.2). Thereafter, an overview of the physicochemical properties of sulfur mustards and their biochemical effects will be provided in order to point to potential paths for its detection (Section 1.3). Then the effects of sulfur mustard on the human body, i.e. the pathophysiology and toxicity (Section 1.4), the acute and delayed clinical symptoms (Section 1.5 -1.7), and options for treatment of the acute and chronic symptoms (Section 1.8) will be given subsequently. Finally, a discussion of the indicators that are used for a differential diagnosis (Section 1.9), and of relevant currently available methods for the detection (Section 1.10) of sulfur mustard exposure will conclude the literature review.

## 1.2 History of Sulfur Mustard as a Chemical Warfare Agent

Historically, the first documented indication for the use of chemicals for warfare dates back to the ancient time. About 600 B.C. the Athenians poisoned the water supply with toxic extracts of the hellebore plant at the siege of Kirrha and could conquer the city thereafter [16]. In 429 B.C the Spartans produced sulfurous vapors/ clouds [20] and more recently Dr. S. James, a professor of Archeology at the University of Leicester, found evidence, that the Persians used chemical weapons in 256. During an attack of a Persian city by the Romans, the Persians used sulphur dioxide and bitumen to create fumes in a tunnel against the attacking Romans. According to Dr. James, the toxic fumes/ gases were the cause of death [22]. Another form of chemical weapons is a poisoned arrowhead. It is known that they were used in America and still are used in areas of South Africa [23] .

Much later, during World War I, CWAs were used at a completely new level as this type of weapon was used after "industrial production" on a large scale by the Germans and subsequently also by the allied forces (Figure 1). Under the scientific lead of Fritz Haber (noble price in chemistry, 1918), the German forces started in April 1915 with a chlorine gas attack near Ypres in Belgium and in July 1917, were the first to deploy bis(2-chloroethyl) sulfide, more commonly known as sulfur mustard (SM), S-Lost or "Yellow-cross" [3,20]. The Allies labelled SM as *Hun Stuff* (HS); the distilled form was called *Hun Stuff Distilled* (HD). Both labels are military designations, which are used until now e.g., in NATO or OPCW documents. Another name, *Yperite*, refers to the city Ypres in Belgium, where it was first used. Moreover, SM was also called S-*LOST* in reference to the two German scientists Lommel and Steinkopf who investigated its synthesis and its potential use in chemical warfare [7,20,24,25].

**Figure 1.** Photograph of German infantry men during a gas attack in WW I. Picture dating 1916/1918, photographer unknown. Reproduced with permission, copyright Bundesarchiv (Bild 183-R05923) [26].

The gruesome effects of chemical weapons could subsequently be seen in various other conflicts. Italy used CWAs between 1935 and 1940 to conquer Abyssinia (present-day Ethiopia) [27]. Japan used them from 1937 to 1945 against the Chinese [27]. Egypt intervened in the Yemenite civil war during 1963 and 1967 by dropping aerial bombs containing SM against the royalist forces [27]. More recently the agents were used during the Iran-Iraq-War between 1983 and 1988, as the Iraqis utilized them against Iranian and Kurdish fighters as well as civilians e.g. in the city of Sardasht

and Halabdscha [2,27–30]. During the current civil war in Syria the use of sulfur mustard was verified with highly sophisticated analytical methods [11,31,32]. Current estimates state that the use of CWA led to about 100,000 deaths and more than 1.4 million casualties since World War I globally [2,33], even though their use was banned in treaties that were signed in 1925 and entered into force on February 8th, 1928, which is now referred to the Geneva Protocols. The initial purpose of the Geneva conference was to establish international law of war. Only later on during the conference of 1925 the use of CWA was banned in war [34] as a direct result of the large scale use of poisonous gases, in particular SM, during World War I and the inflicted enormous suffering and high number of battlefield casualties (Figure 2) [2,35]. However, this Geneva Protocol did not ban the development, production, or stockpiling of CWAs [2,29], which explains the production and further development of them prior to the second world war and during the cold war.

**Figure 2.** Photograph taken during World War I entitled "The blind leading the blind" showing men of the 55th British Division that were casualties of a poison gas attack. Photograph taken on 10 April 1918, photographer unknown. Reproduced with permission, copyright World History Archive (WHA_013_0030) [37].

In 1993 another conference took place, resulting in the Chemical Weapons Convention (CWC), which entered into force on 29 April 1997. As of now, a total of 193 nations are members of the CWC [29], organized in the Organization for the Prohibition of Chemical Weapons (OPCW) as the implementing body in The Hague, Netherlands. In October 2013, after international pressure by the Russians and Americans, the Syrian Arab Republic became a member [36]. The same year the OPCW received the Nobel Prize for Peace for "its extensive efforts to eliminate chemical weapons".

Israel has signed but not yet not ratified the CWC [29]. The main goal of the OPCW is to further the goal of achieving a secure and stable world free of CWAs [5]. The large numbers of soldiers killed and injured as a result of the devastating and indiscriminate use of CWAs led to the classification of agents, e.g. nerve agents or SM, as banned chemicals and their categorization as Schedule 1 CWAs [35]. According to the OPCW, 98.7% of CWAs (as of 31 May 2021) have been in the meantime successfully destroyed under the guidance of the OPCW [5].

Within the medical sciences, research on CWAs was not considered to be of the highest interest and, not least due to the significant safety requirements and the need for laboratories with special licenses, research was undertaken in only a few laboratories worldwide. However, after the Aum Shinrikyo sect employed sarin in Matsumoto (1994) and Tokyo (1995), and following the 9/11 terrorist attacks in 2001, concerns about terrorists using CWAs increased significantly [38]. Moreover, Syrian leaders threatened to use CWAs during the Arab Spring, against their own people as well as intervening countries. The OPCW indeed reported to the United Nations Security Council that civilians were exposed to SM during bombings in 2015, which was confirmed by a team of specialist of the Bundeswehr Institute of Pharmacology and Toxicology in Munich, Germany [11]. However, it remains unclear who deployed SM and some evidence indicates that the terrorist organization "Islamic State of Iraq and Levant" (ISIL) used SM [31,39,35]. Not surprisingly therefore, research on CWAs such as SM has become more urgent again [41].

## 1.3 Chemical and Biochemical Aspects of Sulfur Mustard

The first synthesis of bis(2-chloroethyl) sulfide was reported as early as 1822 by the Belgian-French chemist Depretz and preceded its first use in war by almost one hundred years (Figure 3) [3,6]. In 1854 Riche and in 1860 Guthrie reported on the facile preparation of bis(2-chloroethyl) sulfide by reaction of sulfur halogens with simple olefins and these researchers were the first to note its effects on the human skin [25,42]. Meyer produced pure sulfur mustard and also documented its physical, chemical, and physiological characteristics [3,7,42]. This was considered particularly important for warfare, because contaminated SM carries a distinct smell of garlic or mustard, which can warn enemy troops [7,43]. The use of SM as a military compound and industrial development was investigated by Lommel and Steinkopf [7,24] who showed that even small amounts of bis(2-chloroethyl) sulfide were sufficient to incapacitate and seriously injure many people. The enormous interest in its use for chemical warfare led to the development of an industrial process for its production. Beyond its use as a CWA, however, in 1931 Berenblum and Smith found an anti carcinogenic property of SM in a mouse model [44]. Later on, SM and its derivatives were found to be promising compounds in cancer therapy [7,43]. In consequence, Gilman and Goodmann were the first to explore this approach and contributed substantially to the development of the cytostatic

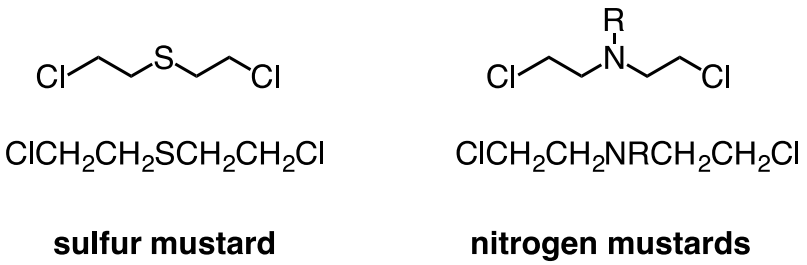


**Figure 3.** Molecular structure formulae and condensed formulae of the chemical warfare agents sulfur mustard and its nitrogen mustard derivatives bis(2-chloroethyl) ethylamine (HN-1) (with R = ethyl), bis(2-chloroethyl) methylamine (HN-2) (with R = methyl), as well as tris(2-chloroethyl) amine (HN-3) (with R = $CH_2CH_2Cl$).

agents [45]. Today, nitrogen mustards (Figure 3) are used for cytogenic treatment, including the derivatives mechlorethamine (HN-2), cyclophosphamide, ifosfamide, melphalan, and chlorambucil [24].

The basis of the manifold dangers of bis(2-chloroethyl) sulfide is to be found in its chemical properties. Obtaining the educts required for the preparation of bis(2-chloroethyl) sulfide and its preparation are comparatively easy. At the same time, the multiple, damaging effects on human beings pose a significant threat to soldiers, first responders, aid workers, and civilians during and, because of its high persistence in the environment, even significantly after an attack with SM has occurred [7]. Additionally, the complexity of the treatment of patients that have been exposed to SM places health care systems under significant strains. Thus, this combination of significant adverse effects, a relative ease of preparation, and its chemical properties renders bis(2-chloroethyl) sulfide a particularly dangerous CWA [46].

### 1.3.1 Chemical Properties of Sulfur Mustard

Pure SM appears as a clear, oily, transparent, almost odorless, and lipophilic fluid at room temperature. Due to impurities from its production the technical grade (Figure 4) form usually used for military purposes looks like a dark and oily appearance with a mustard- or garlic-like odor, which led to the coinage of its name *mustard gas* [15,20,25,38,47]. The vapor pressure of SM is very low (0.11 mmHg at 25 °C) [48] and the freezing point amounts 14 °C. These properties result in a slow vaporization rate at ambient temperature and a long persistency in a cold and dry environment (Table 1) [3,47]. The high freezing point hampered its use as a liquid in combat scenarios. To solve this problem, substances with the ability to lower the freezing point such as chlorobenzene were added to SM. On the other hand, the rate of vaporization in colder climates can be facilitated by combining SM with other vesicant agents that feature a higher rate of vaporization, like 2-chloroethenylarsonous dichloride (Lewisite). This approach was taken by the Japanese army when using CWA against the Chinese during World War II [3].


**Figure 4.** Photographs showing vials with different technical grades of sulfur mustard: On the right, a vial is shown with pure sulfur mustard as a clear, transparent liquid; On the left, a vial is shown containing sulfur mustard as a dark liquid due to impurities from production reaction. Reproduced with permission from Bundeswehr Institute of Pharmacology and Toxicology Munich, Germany [49].

At higher temperatures, the evaporation rate of SM increases [6,15]. The German Chemical Corps used this property tactically to increase the effectiveness during World War I. SM was dispersed at night, when the temperature and rate of vaporization were still low. However, during the morning when the temperatures increased SM started to evaporate to a higher extent. At this time the opponents had already taken off their masks and thus fall easy victims. The vapor of SM has a 5.4 times higher density than air [3]. Therefore, the highest concentrations of SM are typically found a couple of centimeters above the ground, which meant that soldiers were directly exposed to SM in the trenches beside the battlefields during World War I when protecting themselves from bombs and when they left their ditches. This is also important for sampling of air for the process of detection. Samples have to be taken at ground level.

**Table 1.** Overview of relevant physical and chemical properties of the sulfur mustard bis(2-chloroethyl) sulfide [50].

| **Properties of Bis(2-Chloroethyl) Sulfide (Sulfur Mustard)** | |
|---|---|
| **Freezing point** | 14 °C (at 760 mmHg) |
| **Boiling point** | 215–217 °C |
| **Smell** | garlic and mustard-like |
| **Solubility in water** | insoluble (due to lipophilic properties) |
| **Vapor pressure** | 0.11 mmHg (at 25 °C) |

The hazardous effect of as SM as vapor was also used during the Iran-Irak-War. Bombs filled with SM generated an aerosol called “poisonous cloud” [7]. According to Kehe *et al.* [51] Iranian soldiers described those poisonous clouds as grey-blue to black that settled as white dust with an odor of garlic or rotten eggs.

SM is lipophilic and has a high stability (in a water-free setting). It is well-soluble in apolar liquids such as organic solvents, oils, or polymers, but poorly soluble in water [6]. The amphiphilic structure with a hydrophobic and hydrophilic residue leads to the formation of two phases when mixed with water, with SM constituting the bottom phase due to its higher volumetric mass density [6]. At the interphase SM hydrolyzes into thiodiglycol and hydrochloric acid, which leads to the neutralization of SM. The rate of hydrolysis upon stirring in aqueous solutions is dependent on the percentage of chloride ions (chloride ions stabilize SM) and on the temperature. Without stirring or other turbulences hydrolysis is limited to the phase boundary. Especially in chlorine rich environment, e.g. in the Baltic Sea, clots can be formed with the hydrophilic residue outside and the lipophilic residue inside [47]. In this form, SM is quite stable and can persist for a long period of time, e.g. when dumped into the ocean [6] as decomposition reactions run relatively slow, especially at low temperatures [47].

### 1.3.2 Formation of DNA Adducts and Biochemical Aspects

Sulfur and nitrogen vesicants can alter the structure of the deoxyribonucleic acid (DNA) by forming crosslinks within the DNA’s double helix. In particular, these CWAs form bonds with the nucleic acids by undergoing alkylation reactions especially with purines in DNA which are processed to form apurinic sites[52]. DNA adducts can form within the first ten minutes after exposure to SM and its derivatives [52]. Depending on the extent of DNA adduct formation, repair mechanisms are able to restore the DNA. The more substantial the alterations are, the lower are the chances that the repair mechanisms are able to restore the full function of the DNA [53]. The identification of such DNA adducts are a reliable way of detecting the contact with CWAs.

The ability of SM to form DNA adducts originates from the two 2-chloroethyl residues. These residues are electrophilic and as such especially prone to undergo reactions with nucleophilic substances such as thiols, alcohols, carboxylic acids, phosphates, or ring nitrogen’s that are present in DNA, RNA, proteins, carbohydrates, and lipids [25,38,50,51]. The alkylation consists of a two-step reaction. Initially, SM undergoes hydrolysis and an episulfonium ion is formed, which then converts into a carbenium ion (Figure 5a) [7,24]. The episulfonium and carbenium ions are highly reactive species, which lead to the alkylation of the DNA, RNA (Figure 5b) and other proteins. As this thesis refers to DNA damage reactions with other proteins are not considered here.

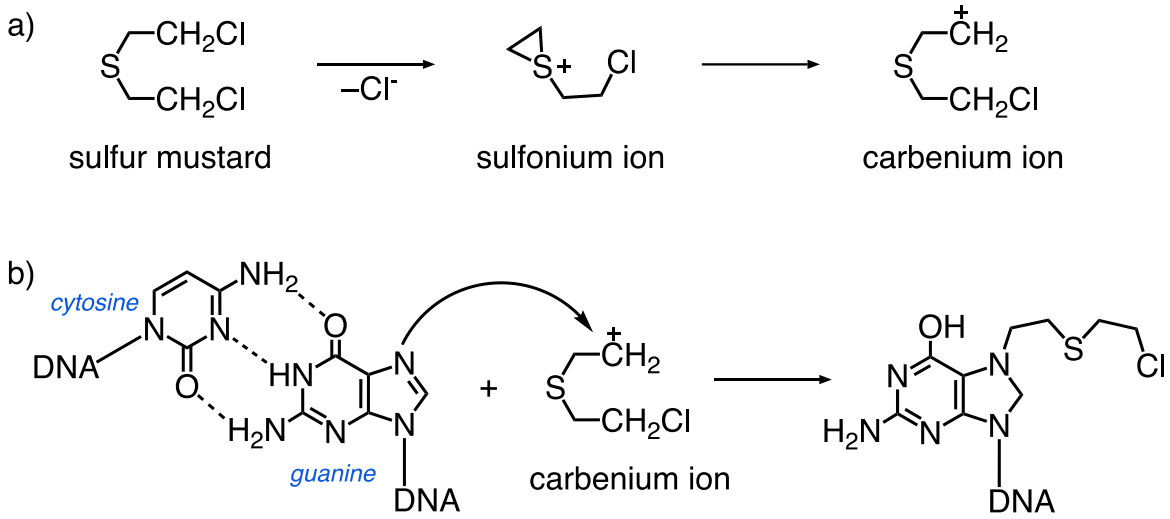


**Figure 5.** Chemical reaction of sulfur mustard with a nucleobase. **a)** In the first step, an elimination of a chloride ion leads to the formation of a sulfonium ion, which can convert into a carbenium ion. **b)** The highly reactive episulfonium or carbenium ions readily reacts with nucleophiles such as in the depicted reaction with the $N_7$-nitrogen atom of the guanine base of the DNA. As a result, a DNA adduct at the $N_7$-position is obtained [24]. In the case of SM, one reactive side chain remains intact after the depicted reaction sequence and the residue can undergo a second alkylation reaction.

If DNA comes into contact with alkylating agents such as SM or its derivatives, different types of alterations to the DNA can occur, categorized as either mono- or bifunctional-type alterations [52]. In the case of SM, a chemical transformation can happen with both 2-chloroethyl residues of the molecule [25,53,54], whereas other mustards such as 2-chloroethyl ethyl sulfide (CEES) that only carry a single reactive residue can only undergo single alkylation reactions (Figure 6) [7]. Compounds that allow two alkylation reactions usually yield bifunctional alterations in the DNA either inter- or intrastrand crosslinks. Interstrand crosslinks are those that are formed by a single bifunctional molecule that reacts with both DNA strands of the double helix, whereas intrastrand crosslinks are formed linkages by a single bifunctional molecule that reacts twice within a single strand (Figure 6c) [7].

Different sites of the nucleobases can undergo alkylation reactions with the highly reactive ionic intermediates obtained after elimination of a chloride ion from SM. The alkylation is particularly often observed at the $N_7$-nitrogen atom of guanine (61–65 %) (depicted in Figure 6), the $N_3$-nitrogen atom of adenine (16–17 %.), the $N_1$-nitrogen atom of adenine, and the $O_6$-oxygen atom of guanine (0.01 %) [24,25,52,53]. Bifunctional cross-links have been found in about 17% of the observed cases and they mostly take place at the $N_7$-atoms of guanine bases [25,52]. Bifunctional alterations in the form of interstrand crosslinks are particularly severe since they can block or stall the synthesis of DNA, RNA, and proteins [6], which may ultimately lead to cell death via disruption of the double helix structure [53,56].

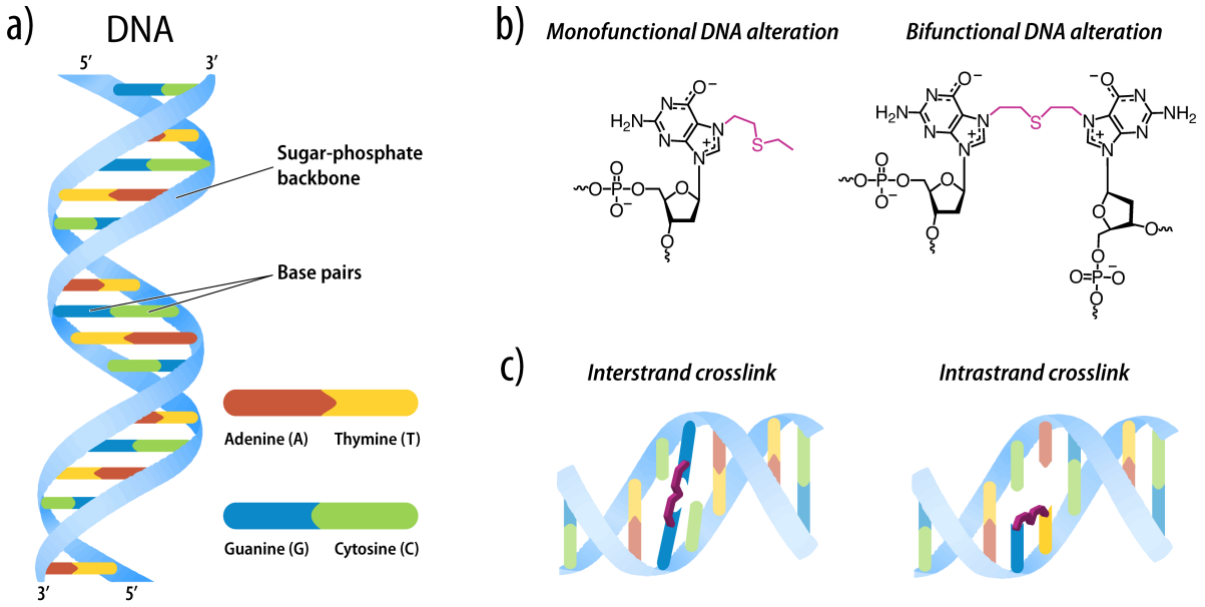


**Figure 6.** Different types of alterations of the DNA. **a)** Schematic depiction of the double helix structure of DNA with base pairs of adenine, thymine, guanine, cytosine, and the sugar-phosphate backbone. **b)** Examples of the molecular structures of mono- and bifunctional DNA alterations. Shown are (*left*) the $N_7$-deoxyguanosin adduct formed by reaction of 2-chloroethyl ethyl sulfide with the guanine base of the DNA and (*right*) the product of a reaction of sulfur mustard and two guanine nucleobases of the DNA [55]. **c)** Bifunctional DNA alterations can lead to the formation of either (*left*) inter- or (*right*) intrastrand crosslinks [6].

## 1.4 Toxicity

To gain an improved understanding of the toxicity of SM, one needs to consider its different chemical and physical properties. For one, there are the above-mentioned aspects of temperature and humidity, which directly influence its reactivity (high temperature and humidity increases reactivity) [3,15,18]. Moreover, the biochemical effects of an exposure to SM only constitute themselves through the delayed occurrence of the first symptoms. The latency period differs for the different tissues, depending on their susceptibility towards SM as well as its distribution [3]. Tissues with a high metabolism rate are more sensitive to SM, for example the eye [57,58] and bone marrow [3].

The amphiphilic nature of SM allows a rapid penetration through lipophilic cell membranes, which is why it can even be found in the brain. Its lipophilic nature enables SM to accumulate in the fat tissue that has a high proportion of lipids. In direct contact with skin, only about 20 % of SM penetrates [6], while the remaining 80 % evaporate. However, SM can cause more damage when warm, moist, and occluded skin areas like the groin are exposed. Thus, the fraction that evaporates is lower and more SM can penetrate the skin layers along the sweat and sebaceous glands [24].

SM can be absorbed via the cornea, skin, and lungs. No data exist for oral absorption. Data for the distribution of SM after exposure differ between data derived from an Iranian soldier and an

experiment on rats. The Iranian soldier, who was exposed to SM and died later on, had the highest concentration of SM in the brain followed by the kidney, liver, spleen, and lung. However, rats that got an injection of radiolabeled SM showed a different distribution with the highest concentration in the kidney followed by the lung, liver, spleen, and brain. Factors that could influence this finding could be apart from the species the route of exposure. The above mentioned Iranian soldier was exposed via skin and the lungs, whereas the rats received it intravenously [59].

SM is metabolized via alkylation, glutathione reactions, hydrolysis, and oxidation. The main metabolite thiodiglycol is found in the urine together with the so-called beta-lyase products. To some degree SM is excreted unmetabolized via the urine and feces. This was found in victims of the Iran-Iraq war [59].

Upon penetration of the skin, SM is able to directly react with various molecules and can even get systemic access. Thus, investigations with terminally ill cancer patients who volunteered to get radioactively marked SM injected showed that the amount of SM that reacts with molecules in the immediate area of penetration is approximately 10–20 %, while the fraction that enters circulation can reach 80–90 % [24]. It was shown that SM left the circulatory system and was excreted via the kidneys within a couple of minutes. The different metabolites of SM such as thiodiglycol sulphoxide, 1,1´-sulphonylbis[2-S(*N*-acetylcysteinyl)ethane], 1,1´-sulphonylbis[2-(methylsulphinyl)-ethane], and 1-methylsulphinyl-2-[2-(methylthio)ethylsulphonyl]ethane were detected in the urine of these patients [24].

The exact mechanism of action is unknown. However, it is thought, that the majority of toxic effects is due to its reaction with the DNA and the formation of inter- and intrastrand crosslinks as well as oxidative stress resulting in tissue damage by reactive oxygen species and potential inflammatory response [60]. The detailed mechanism of action, however, is not focus of this thesis.

The National Advisory Council established special guidelines for SM exposure in cooperation with the Department of Defense and similar institutions [61], which are called “Acute Emergency Guideline Levels” (AEGL). Each AEGL-level creates a relation between the time of exposure (between 10 to 480 minutes), the concentration of SM given in mg/m$^3$ and the possible symptoms that might occur (Table 2). The higher the concentration of SM in a certain area, the shorter is the time of exposure needed to cause the same symptoms compared to a longer time of exposure with a lower concentration in the same area. Three different levels of concentration were defined, at which symptoms with varying intensity occur (Table 2) [3,24,62]. The values for AEGL Level 1 and 2 were derived from volunteers, whereas data for AEGL Level 3 were taken from experiments with mice [59].

**Table 2.** Overview of the "Acute Emergency Guidelines" for sulfur mustard with potential effects depending on the time of exposure and the concentration of sulfur mustard [3].

| Category | Exposure time (min) | Concentration of Sulfur Mustard (mg/m³) | Symptoms | Consequences (late onset) |
|---|---|---|---|---|
| **AEGL-1** | 10 | 0.40 | affection of the eyes (if detectable) | no long-term complications |
| | 30 | 0.13 | | |
| | 60 | 0.067 | | |
| | 240 | 0.017 | | |
| | 480 | 0.0083 | | |
| **AEGL-2** | 10 | 0.60 | irritation of the eye; possibly delayed impairment of vision | no disability; impairment of escape; no permanent or long-term effects |
| | 30 | 0.20 | | |
| | 60 | 0.10 | | |
| | 240 | 0.025 | | |
| | 480 | 0.013 | | |
| **AEGL-3** | 10 | 3.9 | potentially permanent or long-term symptoms of eyes, respiratory system, skin, or systemic effects | incapacitates; need for assistance; potentially lethal |
| | 30 | 2.7 | | |
| | 60 | 2.1 | | |
| | 240 | 0.53 | | |
| | 480 | 0.27 | | |

## 1.5 Clinical Symptoms

As outlined above, SM and its derivatives are classified as vesicant agents because contact to either vapors or direct contact with its liquid forms may lead to blister formation of the skin and mucous membranes [63]. The eyes, skin, the respiratory and gastrointestinal tract, the hematologic system, and the reproductive organs can also be affected [24]. The severity of symptoms after contact with SM or one of its derivatives varies and depends on a couple of factors. The dosage, the duration of exposure, and the susceptibility of the involved tissue influence the appearing symptoms. According to Wattana and Bey the danger of SM arises from four major aspects [3]. The first one is the long period of latency between contact and the first occurring symptoms depending on the site of exposure. The second one is the surrounding temperature and humidity and moisture of the skin, respectively. At higher temperatures moist skin is prone to be sufficiently damaged by lower amount of SM. The third aspect refers to the differing sensitivity of the affected tissues after contact with SM. Thus, thin, warm, and moist skin is more sensitive towards SM than thicker and

less moist skin. For example, skin at the axilla and genitals is more susceptible than skin at the forearm. Finally, the fourth point refers to the amount of SM, one had contact with.

The concentration of SM that is needed to induce blister formation on the skin lies between 100 µM and 1 mM or between 1.0–2.5 µg of SM per square centimeter of skin area [64]. Different concentrations are reported for direct contact with the liquid or vapor of SM. The liquid form of SM causes blister formation with $10 - 20\ \mu g/cm^2$ and the vapor shows similar effects at $1000 - 2000\ mg/m^3$ [53].

At the AEGL-1 no consequences or no residuals are seen after contact to SM. If symptoms occur, they are mainly conjunctivitis at the eye. At AEGL-2 other organs such as the skin and respiratory system are affected, as well. Severe conjunctivitis, photophobia, eyelid swelling, and blister formation at the skin can occur. Usually, no long-lasting effects occur at this level. At the third level, an acutely life-threatening situation is at hand and long-lasting residuals can occur.

After having contact to a chemical warfare agent like SM, the consequences for human beings are complex and severe. In the following paragraphs the acute and chronic effects of the different affected systems after contact to SM will be explained in detail.

## 1.6 Acute Effects

Acute effects after exposure to SM mainly affect the eyes, skin, and respiratory system. Later, the organ systems are affected as well. The eyes are highly susceptible towards SM due to the moist environment and easy accessibility [3,6,24,62]. The skin and respiratory system have a higher latency period until they show the first symptoms.

### 1.6.1 Symptoms of the Eye

The high susceptibility of the eye is a result of the anatomy of the cornea and the mucosa of the conjunctiva as well as the high intrinsic metabolic activity and high cell turnover rate of the eye [6,27]. Especially the interface between the cornea (with a high proportion of water) and the mucosa of the conjunctiva constitutes an excellent surface for easy and fast penetration of SM. Additionally, the aqueous cornea provides an optimal surface for hydrolysis of SM with the formation of caustic hydrochloric acid. Hydrochloric acid causes additional irritation and damage to the surface of the cornea and conjunctiva, facilitates penetration of SM into the tissue. This process results in apoptosis of corneal and conjunctival cells.

Depending on the duration of exposure and concentration of SM, a variety of symptoms of different severity can be observed [27]. Acute symptoms usually occur between 30 minutes and up to 8 hours after exposure [3,27,51]. They include photophobia and a phase with acute injury of the eye

(inflammation of the anterior segment of the eye and corneal erosions). The typical long term effects occur later on, often after years and sometimes even after a long lasting clinically unapparent phase [65]. These features are discussed in the paragraph of chronic symptoms.

Mild symptoms can occur at a concentration of 50–100 mg · min/m$^3$ of SM vapor and include sicca symptoms (the feeling of a foreign object sensation, conjunctivitis, tearing, dryness, and pain) [6,24]. These tend to completely resolve. Exposure to concentrations of more than 200 mg · min/m$^3$ can lead to moderate symptoms that are more intense with blepharospasm, photophobia, corneal edema, and chemosis (but also vesication of the cornea with sloughing and a decrease in visual acuity) [6,24,27]. If the eyes are examined with a fluorescing agent, erosions of the cornea of varied size can be seen. Severe symptoms are observed after exposure to vapor concentration of above 400 mg · min/m$^3$ or direct contact with SM [24,27]. This can result in an inflammation of the anterior chamber of the eye with danger of blocking the drainage of the intraocular fluid, which can cause an acute increase of the intraocular pressure with the risk of acute glaucoma. If limbal vessels are affected a decrease in nutritional supply of the cornea can occur and an increase in the release of vascular proliferative substances, leading to the neo-vascularization of the cornea and later on the formation of pannus [24]. If the small limbal vessels become necrotic, whitening of the temporal and nasal limbus can occur, as seen after contact with an acid or base. Larger necrotic lesions and perforation of the cornea may result in symblepharon. Moreover, even the eyelids can be affected and the development of up to second-degree burns have been described [3,24].

### 1.6.2 Symptoms of the Respiratory System

The respiratory system can be affected after inhalation of SM. First symptoms usually occur between 4 to 16 hours after exposure and are caused by irritation of the mucus membranes, and include edema and erythema down to the terminal bronchioles [3]. The effects on the respiratory system are thought to influence the course of healing the most and might lead to a fatal result, which will be explained below [62]. Two important factors influence the severity of these symptoms. One of them is the duration a victim was exposed to the vapor of SM and the second one is the amount of SM, which was inhaled. This mostly depends on the number of breaths taken per minute and the depth of respiration. The higher the respiratory rate and depth of respiration, the more severe the symptoms [3,24].

Lower concentrations of SM normally lead to pain and a burning sensation in the nasal region which are usually accompanied by sneezing, a sore throat, and rhinorrhea [3,6]. This can already occur at vapor concentrations of 12–70 mg · min/m$^3$ [51]. Higher concentrations and an increasing amounts of inhaled SM lead to more severe symptoms such as tracheobronchitis with a dry cough and aphonia, edema of both the upper and lower airways, formation of pseudomembranes, as well

as ulcerations and necrosis of the respiratory epithelium (including the larynx, trachea, and bronchia) [3,6,24,51], which all adds on to the symptoms mentioned above. The pseudomembranes can cause severe obstruction of the airways leading to respiratory complications with obstruction of the upper and lower airways [3,6]. The need for intubation might occur. Pseudomembranes can irritate the vagal nerve and cause reflex-asystole [3,24].

The formation of ulcerations and necrosis facilitates the penetration of the respiratory mucosa by germs significantly increasing the chances for subsequent infections. One of the most involved and feared bacteria is Pseudomonas aeruginosa [3] which may aggravate the patients' situation by bronchopneumonia especially in intubated patients. Within 36–48 hours after initial exposure, severe inflammation and even necrosis of respiratory tissue with bronchopneumonia can occur [3,6]. The time of recovery ranges between one to two months and mostly depends on the degree of damage to the respiratory system and the resulting complications [3].

### 1.6.3 Symptoms of the Skin

Vesicating agents like SM and its derivatives affect the skin in a typical way with symptoms observed after exposure to vapors or liquids. The temperature, moistness, duration of exposure, and concentration influence the development of the symptoms [6,7,20,24,53]. Haber´s Rule of correlation between the concentration of an agent and the time of exposure can be applied. Thus, contact with a high concentration of an agent for a short period results in the same symptoms as exposure to low concentrations of the same agent for a longer period [24,53,62].

As outlined above (Section 1.4), SM and its derivatives penetrate better into warm and moist skin. Thus, areas of the body with thin-layered skin, high density of sweat glands including the inguinal, genital, and anal region are more susceptible [3,20,27,51,62,63]. First symptoms usually occur within 2–24 hours after exposure and normally include erythema, and pruritus (vapor 100-300 mg · min/m$^3$; liquid 10–20 µg/cm$^2$), as well as a burning sensation, and formation of vesicles (vapor 1000–2000 mg · min/m$^3$; liquid 40–100 µg/cm$^2$) [6,63]. The vesicles usually appear about 18 h after first contact to SM within the area of erythema and can become bigger (progress into blisters) and coalesce and slough (Figure 7). The blisters typically contain a yellow fluid, which is not toxic [3,24,51]. If the blisters break erosions, loss of the skin, ulcers, and even necrosis can develop (Figure 8) [6,27,51,53,63]. The areas of necrosis can form eschars (around 72 h post exposure) [6,25].

### 1.6.4 Systemic Symptoms

The occurrence and extent of systemic symptoms depends on the absorbed amount of SM and its distribution across all organs. Systemic consequences are similar to those arising of chemo- and radiotherapy. This includes headache, gastrointestinal symptoms (nausea, loss of appetite,

diarrhea, cachexia, and vomiting), affection of the bone marrow (immune suppression, leucopenia), and the psychopathological and neurological symptoms (decreased concentration, vitality, libido, and potency; neuralgic complaints, depression, apathy) [3,6,7,51]. The psychopathological and neurological effects were observed by Iranian soldiers that showed signs of apathy and depression after exposure and similar effects were seen in German factory workers who produced SM-based CWAs [7,51].

**Figure 7.** Photograph of a victim of sulfur mustard exposure showing hypo- and hyperpigmentation of the skin on the back. Reproduced with permission from reference [51], copyright Elsevier.

The effect on the bone marrow is variable and mostly depends on the amount of absorbed SM, with lower concentrations leading to leukocytosis, while higher concentrations cause leucopenia. The alkylating properties of SM particularly affect tissues such as the bone marrow with a high cell turnover and rapid proliferation rate [3,15]. Initially, the cell number is decreased and atypical precursors of the erythropoietic cell line occur in the peripheral blood. Leukocytosis typically occurs during the first 3–5 days after exposure, which can thereafter turn into leucopenia (erythropoiesis and megakaryocytes can also be affected, leading to impaired hemostasis with increased risk of bleeding) [3,6,7,20,24,27]. Leucopenia results in a higher susceptibility to secondary

acquired infections with a high mortality rate. A cell count that is lower than 200 cells/mm$^3$ goes with the highest probability of death [3,6].

**Figure 8.** Photograph of the skin of a victim of sulfur mustard. Little blisters, larger bullae, and erythema of the skin are observed in the areas that were exposed to SM. Reproduced with permission from reference [51], copyright Elsevier.

## 1.7 Chronic and Delayed Effects

Following acute effects caused by SM and its derivatives, chronic effects and nasty residuals can occur. Symptoms of these chronic and delayed effects are predominantly found on the same sites as during the acute phase of intoxication, i.e., on the skin, in the respiratory system, the eye, the bone marrow and the blood system. Exposure to a hitherto inviolate area may even result in re-occurrence of signs and symptoms at skin areas which have been affected long ago. Their severity mostly depends on the amount of SM exposure, the time of exposure, especially in occupational exposure [3,6,24,66].

### 1.7.1 Symptoms of the Eye

Exposure of the eyes to SM can cause long-term sequela. The cornea is sensitive towards SM and the corneal stem cells at the limbus of the cornea can be damaged, which can cause late-onset symptoms. A characteristic SM induced long-term effect is the late-onset ulcerative keratopathy, which may occur about 15–20 years after initial contact [6,67]. Ulcerative keratopathy is characterized by an infliction of visual accuracy, photophobia, and lacrimation. On slit lamp examination the eye typically shows thinning, opacification, and neo-vascularization of the cornea and a deficiency of corneal stem cells at the limbus, which leads to a deficient production of

corneal cells [6,24,27]. If the corneal epithelial cells decrease, a defective cornea with persistent and progressive destructive keratitis is caused. The protective properties of the cornea are decreased, rendering it more prone to infections and scarring because of an uneven surface and an increased risk of perforation [3,67]. The most severe ocular complication after exposure to SM is blindness [68].

Another symptom that might occur is chronic blepharitis (inflammation of the edge of the eyelid), which is caused by an obstruction and inflammation of the Meibomian glands and the resulting dry eyes [3].

### 1.7.2 Symptoms of the Respiratory System

The severity of acute symptoms of the respiratory tissue can vary as mentioned above. After initial rehabilitation from acute effects, victims, and also initially asymptomatic victims can develop chronic symptoms even years after exposure [3]. Frequently described symptoms are dyspnea, a chronic cough, and an increased mucus production. On physical examination wheezing, crackles, decreased breathing sounds, clubbing of the fingers (sign of chronic hypoxemia), and cyanosis were observed [3,6,67]. Victims also showed an increased reactivity of the respiratory system, chronic bronchitis with recurrent infections, asthma, bronchiectasis, narrowing of the large airways, and pulmonary fibrosis [3,6,24,27].

Acute affection of the upper airways can subsequently lead to the formation of scars, fibrosis, and mucociliary dysfunction with inadequate outward transportation of cell debris and mucus. Moreover, the disturbance of the protective properties of the mucociliary apparatus may lead to recurrent infections. This can cause stenosis of the trachea and bronchi (narrowing of the large airways) [6,27,67].

However, the major pathologic process affects the lower respiratory system, i.e., the lung. Bronchiolitis obliterans is most frequently diagnosed. It is verified by high-resolution computer tomography scan, bronchoalveolar lavage, and lung biopsy [67]. The computer tomography scans of victims of SM exposure showed air trapping, bronchiectasis, irregularities and dilation of the major airways, and thickening of the bronchial walls as well as the interlobular septs [24]. Bronchiolitis obliterans leads to scarring and loss of the bronchioles, and ultimately to the formation of bronchiectasis and obstructive lung disease. These direct effects of SM on the respiratory mucosa cause recurrent respiratory infections [6].

Bronchoalveolar lavages (BAL) showed increased levels of the transforming growth factor beta (TGF-beta), which is usually found in fibrogenic disorders [24]. It was found, that SM can also cause pulmonary fibrosis, which is thought to develop in patients with recurrent inflammatory processes of the small airways [6,24].

In general, a huge number of patients who suffer from chronic respiratory disease are unfit to work and require support. At present about 64000 victims of the Iran-Iraq war are monitored closely. Of the 64000 about 24000 developed lung injuries [66]. How many victims of SM receive compensation is not exactly known. Moreover, studies with veterans of World War I and factory workers concluded that repetitive and long term exposure to SM could lead to an increased risk of lung cancer [3,69].

### 1.7.3 Symptoms of the Skin

While minor or mild acute cutaneous alterations of SM exposure generally heal, although with a delay, sites with more severe symptoms, e.g., formation of blisters and necrotic wounds, are at risk of developing chronic wound healing disorders and residuals. Dry skin, pruritus, burning sensations, pain, erythema of previously affected areas, desquamation, hyper- and hypopigmentation – so called poikiloderma -, cherry angioma, atrophic skin, and scar formation are common long-term residuals [3,6,15,24,27,67,70]. The scar formation appears to be due to an increased and uncontrolled activity of fibroblasts, which typically appears when the dermal layer was affected by SM and necrosis occurred [67]. The scars can be either atrophic, hypertrophic, or may display an increased formation of keloid [67].

Melanocytes are responsible for the pigmentation of the skin and disturbance of their function may result in hypo- or hyperpigmentation. When melanocytes are destroyed hypopigmentation usually occurs in the afflicted areas. By contrast, hyperpigmentation develops in areas in which the melanocytes were damaged by inflammation, but not destroyed (Figure 9) [24]. Pruritus, burning sensation, and desquamation typically appears at sites with dry skin, which explains why these symptoms worsen in dry climates [6]. Affected areas are mainly found in the axilla, face, and genitals [3]. As mentioned above, SM-penetration is enhanced in these regions, which are therefore at increased risk of developing more severe symptoms, including sequelae. Some victims even developed chronic eczema, seborrheic dermatitis, and urticaria [67]. Seborrheic dermatitis was accompanied by atrophy of the skin, post-inflammatory hyperpigmentation and alopecia (loss of the hair) in the affected areas.

While some symptoms tend to worsen, others regress in their severity. Especially dryness of the skin and consecutive pruritus are amongst the symptoms that worsen over time. The chronic wound healing disorders are thought to be due to a senescence of mesenchymal stem cells and therefore a reduced migration and wound healing [70].

**Figure 9.** Hyperpigmentation of the skin that was exposed to sulfur mustard during an attack in the Iran-Iraq war. The non-affected areas were protected by a belt worn during the time of exposure. Reproduced with permission from reference [24], copyright Elsevier.

Even though SM is a known carcinogen, no correlation between exposure and increased risk of cutaneous cancer could be found after only a short one-time exposure [3]. While the time between exposure during the Iran-Iraq war and the study of victims might not have been enough to allow for final conclusions, Iranian soldiers that were exposed to SM reportedly developed cutaneous malignancies exclusively at sites of previous contact to SM [67].

### 1.7.4 Systemic Symptoms

The immune system can also be affected by SM and its derivatives, especially in the time-frame after initial exposure. Blood samples of exposed people showed leucopenia. However, in long-term follow-up studies no significant changes were observed. Only a small number of victims with severe affection of the respiratory system displayed a decrease in natural killer T cells [6,27]. Some victims suffered from psychological problems such as depression, anxiety, and posttraumatic stress disorder symptoms. While it is difficult to differentiate whether these problems were effects of general stress arising during war, or a result of the particular exposure to CWAs, there was a higher rate of such complications in people exposed to CWAs compared to victims of war without involvement of CWAs [27,67].

### 1.7.5 Delayed Effects after Exposure

Years after exposure victims can experience delayed effects such as a development of corneal scarring, dry eyes, a chronic cough, hypersalivation, asthma, emphysema, lung fibrosis, Gastro-Esophageal-Reflux-Disease, and scaring of the skin. The scaring can lead to contractures with deformations. One can also find a higher rate of lung and laryngeal caner, multiple skin tumors,

and chronic myeloid leukemia [6].

## 1.8 Treatment of Acute and Chronic Symptoms

General steps that should be undertaken immediately after exposure to SM and its derivatives include a thorough decontamination to stop the penetration of the skin barrier by these CWAs, the monitoring of fluids and electrolytes balances, as well as the detection of possible acute problems arising from exposure to SM and its consequences [6]. The three main organs affected and those that need to be closely examined are the eyes, the skin, and the respiratory system.

### 1.8.1 Decontamination

The goal of decontamination is to prevent further absorption of SM and its derivatives into the skin as well as ensuring that no additional contamination occurs [20]. The first and most important treatment after cutaneous exposure to SM is the disposal of clothing to prevent any further contact with SM and reduce potential damages to the skin. This should be directly followed by a decontamination with special agents such as the Canadian *Reactive Skin Decontamination Lotion Kit* marketed by Emergent BioSolutions Inc. or Fuller´s earth (United Kingdom). The US army uses decontamination kits (e.g., M291 skin decontamination kit) that allow for the physical removal, absorption or neutralization of vesicant agents. If all the above-mentioned agents are unavailable, one can use talcum powder or flour (not to be used for wounds and eyes). Alternatively, one can wash with copious amounts of water and soap [15,18,63,71,72] over a period of at least 15 minutes. It is recommend to wash with copious amounts of water and thereby avoiding harsh jets, in order to minimize possibly destroying the skin barrier and preventing penetration of SM into the skin [24,72]. Notably, however, water from puddles or rivers near the areas of exposure should be avoided, as these might also be contaminated [51], with the danger of further exposure and more severe lesions. If water is unavailable fresh 0.5% hypochlorite solution or household bleach can be used [19,20,63]. However, it should be taken into account that hypochlorite can lead to side effects on the mucous membrane and the eyes [71,73].

### 1.8.2 Treatment of Cutaneous Symptoms

**Pruritus.** As already mentioned, pruritus occurs as one of the symptoms after contact to SM vapor or after direct cutaneous contact. This can be controlled via symptomatic treatment with antihistamines. Wattana and Bey alternatively recommend a mixture of 1% phenol combined with 1% menthol to control the pruritus [3]. Pruritus is also among the chronic symptoms and soothing creams and emollients can be applied externally in addition to the prescription of orally administered antihistamines [67].

**Pain and Chemical burns.** Chemical burns are painful and therefore treated with a variety of analgesics depending on the degree of pain. Light pain is treated by analgesics while opioids, oral narcotics, or systemic analgesics are used to control more severe pain. In all cases, cooling of the affected areas can be performed additionally [3,63]. Chemical burns cause an inflammation of the skin and, according to Ghabili *et al.* [27], SM-induced inflammations could be antagonized by glucocorticoids and non-steroidal anti-inflammatory drugs. The burns reduce the protective quality of the skin barrier, which results in a less efficient defense against microorganisms. This can cause infections of the affected area, especially in the case of chemical burns caused by SM that has also immunosuppressant properties on the bone marrow [6].

**Bullae.** Injuries following the formation and rupture of bullae need sterile dressing, application of topical antibiotics, or the use of silver sulfadiazine to prevent or treat cutaneous infection. The cutaneous defects take longer to heal. In order to expedite this process and to allow assessment of the wound ground it is recommended to open and drain the bullae under clinical conditions [3].

**Wound Healing.** In order to promote the process of healing atypical cells should be removed. This procedure can be done surgically or, e.g., by a carbon dioxide laser. These approaches are currently used in research and not universally available for general treatment for SM induced skin defects [3]. Also, the application of hydrogels and hydrocolloids has been reported to shorten the time of healing [63].

### 1.8.3 Treatment of Respiratory Symptoms

Several symptoms and complications can arise after inhalation of SM and all of them need treatment. First, adequate ventilation of the lungs needs to be secured and victims have to be removed out of danger zones [6]. SM causes irritation and inflammation of the respiratory tissue, which can cause coughing and swelling of the membranes, which in turn can lead to difficulties in breathing accompanied by laryngospasm [24]. Coughing should be suppressed with antitussives, because it may further irritate the affected respiratory tissue and can lead to a decrease of oxygenation. To circumvent this, oxygen should be administered in combination with moistening of the airways to decrease the irritation of breathing dry air [6,20,24]. Bronchospasm and laryngospasm can also lead to difficulties in breathing with stridor and hoarseness. Inhalation of bronchodilators and corticosteroids can alleviate these symptoms. However, if the symptoms persist, assisted breathing devices can be used or intubation or tracheotomy might become necessary to secure adequate ventilation [20,24,63].

As mentioned in the previous chapter, exposure to high concentrations of SM can lead to severe damage of the respiratory tissue with sloughing of the tissue and formation of pseudomembranes. These can obstruct the airways, make breathing difficult, and can lead to irritation of the vagal

nerve with reflective decrease in heart rate and even asystole. If the patient already has a tracheostoma, the pseudomembranes as well as cell debris can be removed with a bronchoscope [3,20]. Otherwise, it is advisable to create a tracheostoma, because severely damaged respiratory tissue calls for repeated bronchoalveolar lavage, which is much easier via the stoma. Additionally, adequate oxygenation can then be secured through mechanical ventilation via the stoma[3,24,53]. However, studies by L. Veress et al. show promising results in a rat model. The tissue Plasminogen Activator was applied to rats after they were exposed to CEES. The group that received tissue Plasminogen Activator had a better survival rate than the other groups. It is thought, that the tissue Plasminogen Activator dissolves cells debris/ pseudomembranes and optimizes varies factors [74].

The suppression of the immune system that is caused by SM exposure may increase the risk of an infection of the airways. This can cause pneumonia, which needs to be treated with antibiotics [3,6,15,24,67]. After rehabilitation of the acute effects, victims can develop sequelae including chronic bronchitis and bronchiolitis obliterans [67]. For treatment, inhaled corticosteroids, anticholinergic agents, and beta-2-agonists were found to improve the pulmonary function [3,6,20,67]. In cases of bronchiolitis obliterans refractory to therapy, immune modulating medications such as interferon gamma can be prescribed [3,24,27,67].

### 1.8.4 Treatment of Ocular Symptoms

The eyes should be decontaminated by washing with copious amounts of water or 0.9% buffered saline [6,63]. Other approaches can only alleviate symptoms. To treat and ameliorate pain, soothing eye solutions are applied into the eye. Damage to the eye with conjunctivitis, pain, and blepharospasm can cause increased secretion of inflammatory fluids, which contains fibrin. This can cause adherence of the eyelids. In order to prevent this, sterile Vaseline can be applied to the eye [72]. A super-infection of the eye with the risk of even more severe damage and risk of losing the eye-sight should be prevented by application of antibiotics as well as corticosteroids, and cycloplegics can be additionally applied intraocular [3]. The corticosteroids prevent an excessive immune answer to inflammation and the risk of late-onset neovascularization can be reduced, which could worsen the condition of the eye [3,75]. In cases of severe damage to the cornea and visual impairment, corneal transplantation as well as amniotic membrane transplantation should be considered [3,75]. However, both approaches remain controversial [68,75]

### 1.8.5 Treatment of Systemic Effects

Systemic effects after exposure depend on the amount of absorbed CWA, its access to the blood stream, and systemic distribution beyond the initial site of contact. As mentioned above (Sections

1.6.4 and 1.7.4), systemic symptoms after contact with SM or its derivatives can mimic the symptoms of chemo- and radiotherapy, including immunosuppression, diarrhea, and nausea, amongst others. The leukocytes (or white blood cell (WB(C/count)) will start to drop on day three and reach its nadir between seven and nine days after exposure [24]. When the leukocytes are below a threshold in the peripheral blood, the physiologic bacteria within the gastrointestinal tract can become a potential source for opportunistic infections in an immuno-suppressed individual. Wattana and Bey recommend a prophylactic administration of antibiotics in patients with a WBC below 200 cells/$mm^3$ to sterilize the gastrointestinal tract and prevent a spreading of opportunistic infections from the bowel. A different option to cope with SM-induced leucopenia would be to consider giving granulocyte-macrophage colony-stimulating factor (GM-CSF) and granulocyte colony-stimulating factor (G-CSF) [3].

To treat nausea and vomiting, metoclopramide or hydroxytryptamine-3 (HT3)-receptor antagonists like ondansetron can be given [24]. As described in Section 1.3.2, $NAD^+$ is depleted in SM exposed cells, leading to necrosis. This could be prevented by blocking the PARP enzyme with nicotinamide [24]. Thus far, however, treatment with nicotinamide is still in the experimental stage and therapy remains symptomatic with no specific antidotes. Experiments by Balszuweit *et al.* have shown promising results in treating SM-exposed HaCaT cells with *N*-acetylcysteine [76]. In order to explore the potential benefits of an improved and tailored therapy, exposure to SM needs to be demonstrated and fast detection methods are accordingly very important.

## 1.9 Differential Diagnosis

The symptoms that are observed in the aftermath of a SM intoxication show a huge variance, but in their entirety appear to be quite specific for this substance. There are general differential diagnoses that should be considered, e.g. the blister formation which can occur after plant poisoning [77]. Blister formation is also possible after exposure to nitrogen mustards, organic arsenicals like Lewisite, and phosgene oxime [15]. While nitrogen mustards are closely related to the sulfur derivatives, phosgene oximes are a bit different in their clinical presentation [24]. The latter lead to urticaria–like cutaneous changes instead of vesical and blister formation, but they are still counted among the vesicant agents.

The characteristic garlic-like odor can also be caused by several other agents including arsenic, selenium, thallium, and organophosphates [15]. However, exposure to these substances is accompanied by symptoms of the gastrointestinal tract like nausea, vomiting, and diarrhea with complications such as loss of volume, metabolic acidosis, and coma. Organophosphates can additionally cause typical cholinergic symptoms, which include abdominal cramps, bronchospasm, miosis, salivation, sweating, bradycardia, tremor, weakness, and fasciculations [15].

In a patient with suspected intoxication with SM, an additional intoxication with Lewisite should always be considered as the latter was often used to decrease the freezing point of SM and increase its effects in colder climates (see above). Lewisite forms cyclic thioarsenite complexes after reaction with vicinal thiol (sulfhydryl) groups [24]. The differentiation between a SM and Lewisite exposure is challenging. Thus, blood and urine samples need to be collected and analyzed in special laboratories, which are able to detect the different metabolites, educts or adducts by using advanced analytical methods [15,78]. The forensic process of confirmation requires sophisticated, high-end methods, which are at present only available in 18 laboratories worldwide, which are designated by the OPCW [79].

## 1.10 Available Methods of Detecting Contact to Sulfur Mustard

The detection of CWAs is more important than ever with continued terrorist threats around the globe [38] and, for example, the ongoing civil war in Syria, in which rebel troops and the regime are suspected of repeatedly using CWAs [80]. To unambiguously prove the use of CWAs laboratory tests are required. On the one hand it is necessary to detect SM within the environment and on the other hand to be able to detect actual exposure to SM.

SM and its derivatives are classified as Schedule 1 (nerve agents, vesicants) CWAs that have electrophilic properties [29,38]. Such electrophilic agents are able to hydrolyze, metabolize, or bind to nucleophilic sites of macromolecules like the DNA or proteins, and the products of these reactions are called adducts [38]. Current detection methods are based on mass spectrometry and on immunochemical analyses.

Metabolites of SM can be detected in the urine. One of them, thiodiglycol, can be observed up to two weeks after contact. However, small amounts of thiodiglycol are also found in unexposed subjects [4,38,81], impeding verification. Further metabolites of SM are formed via the β-lyase/glutathione pathway, i.e., 1,1-sulfonyl-bis[2-methylsulginyl)-ethane] and 1-methylsulfinyl-2-[(methylthio)-ethylsulfonyl]ethane, which can be used for analysis [81].

Beyond the presence of these metabolites, the adducts formed upon exposure to SM can be identified and used as a detection method to recognize cases of SM exposure [24,78,82]. Adducts of hemoglobin [83] or albumin [41,78] can be directly detected by mass spectrometry after derivatization with methods such as GC-MS [83], LC-ESI-MS-MS [41], or μLC-ESI MS/MS [78]. Moreover, immunochemical methods have also been described as a suitable technique for the detection of SM-adducts of proteins and the DNA [24,55]. The adducts of SM have a longer half-life than SM itself, which extends the period of time in which exposure to SM can be detected by this method [38].

Environmental samples are more diverse (air, soil, and water). After SM had contact with different

substances it might already be degraded. For this environmental samples potentially require detecting different substances in order to detect possible use [59].

## 1.11 Scope of this Thesis

The outlined dangers of SM and its derivatives necessitate the development of a reliable and fast method of detecting exposure to such agents, suitable to be used already in the field without the need to deploy sophisticated laboratory technologies. Thus, the aim of the present thesis is to investigate and optimize a protocol that has been based on a detection method previously reported by van der Schans and coworkers ("Standard Operating Procedure for Immunoslotblot Assay for Analysis of DNA/Sulfur Mustard Adducts in Human Blood and Skin") [55]. The method under investigation is expected to allow for a fast detection of the DNA adducts that are caused by reaction with bis(2-chloroethyl) sulfide and its different derivatives in human immortalized keratinocyte (HaCAT) cells. At some point there already existed a test kit to quickly detect sulfur mustard in the environment. However, at the moment - for unknown reasons - it is not functioning anymore, which is why further testing for the test kit needs to be undertaken.

The main goal of the present thesis is the detection of the DNA adducts by using the primary monoclonal antibody 2F8 (2F8 Antibody purified Ab 246, 1.05 mg/mL, BBI Dundee), which binds to adducts formed by sulfur mustard and its derivatives. To that end, immortalized human keratinocytes were chosen because they are relatively easy to nourish and grow, and these cells will be exposed to the chemical warfare agents sulfur mustard (SM), semi mustard (2-chloroethyl ethyl sulfide, CEES), as well as the nitrogen mustards bis(2-chloroethyl) ethylamine (HN-1), bis(2-chloroethyl) methylamine (HN-2), and tris(2-chloroethyl) amine (HN-3). The effects of exposure will be studied by employing the above-mentioned methodology in search for the formation of DNA adducts. In particular, the use of different dyeing methods will be explored and the results regarding the limit of detection will be compared to the method by van der Schans and coworkers in an attempt to optimize the visualization of DNA adducts caused by SM and its derivatives.

# 2

# Outline

# 2 Outline

The possible dangers and effects of CWAs such as SM on human beings – somatically and psychologically – were outlined in the preceding introduction. Current events as in Syria showcase the danger of CWAs and underline the importance of detecting exposure to CWAs in general, and SM as well as its derivatives, in particular. The exposure of human tissue to SM causes DNA alterations in the form of DNA adducts. These adducts can be detected by the primary antibody 2F8, and a methodology was developed by van der Schans *et al*. that exploits the antibody 2F8 to detect DNA adducts that originate from SM exposure [55].

In the context of the present thesis, the developed methodology will not only be further optimized for the detection of SM, but the utility for the detection of DNA adducts caused by different other derivatives of SM such as CEES, HN-1, HN-2, and HN-3 will be investigated. Additionally, attempts will be undertaken to decrease the required amount of DNA and further improve the sensitivity of the test methodology to DNA adducts caused by these agents. Moreover, with the goal of developing a field-test kit that allows for a fast detection of exposure to SM and its derivatives, a streamlining of the process of detection will be investigated.

# 3

# Materials

# 3 Materials

0.05% Trypsin-EDTA: GIBCO® invitrogen

2-Chloroethyl ethyl sulfide (CAS-No. 693-07-2)

2-Propanolol

2/4 Digital: IKA® MTS, Staufen

2F8 Antibody purified Ab 246, 1.05 mg/mL: BBI Dundee

3,3'-Diaminobenzidin (DAB) color and stock solution (+ Glucose Oxidase)

70% Ethanol

AndorIQ 1.9.1, Bioimaging

Antibody Diluent with Background reducing Components: Dako®

Bis-(2-chloroethyl) ethylamine (CAS-No. 538.07.8)

Bis-(2-chloroethyl) methylamine (CAS-No. 51-75-2)

Bis-(2-chloroethyl) sulfide (CAS-No. 505-60-2)

Blotting Unit SHM-48

Cell Counter + Analyser System Model TTC: CASY® Schärfe System, Innovatis, Reutlingen

Centrifuge 5415 R: eppendorf, Hamburg

DMEM (Dulbecco´s Modified Eagle Medium) 41966: GBCO®Cell Counter Analyser Sytem, Model TTC: CASY® Schaerfe System, Innovatis Casy Technology, Reutlingen

Hera cell: Thermo Scientific, Harnau

Heraeus Thermo Scientific, Kendro Laboratory Products, Harnau

HRP-Enzyme: Dako® ADVANCE™

HRP-Link: Dako® ADVANCE™

Image J 1.42q, Wayne Rasband, NIH, USA, rsb.info.nih.gov/ij

Image Scanner III: GE Healthcare

IrfranView Version 3.98: Irfan Skiljan, Wiener Neustadt, Austria

LabScan™ 6.0 Powered by melanie™, © Swiss Institute of Bioinformatics

Li-COR: Biosciences, Hamburg

Melphalan AIC Amp 4142, 10 µg/mL

Melphalan AIC MP 5173, 10µg/mL

Model TTC, Cell Counter Analyser System: CASY® Schärfe System, Innovatis Reutlingen

MSpA1, Multi Core™, Bovine Serum: Promega corporation, Madison, WI

Nitrocellulose Transfer Membrane: Protran BA 79, Pore size 0.1 µm; Whatman®, PROTRAN®

Nuclei Acid Sample Loading Buffer, 5x; EZ Load™ 100bp Molecular Ruler 50µg/mL: Bio RAD

Odyssey

PASW Statistics Version 18

peq GOLD Universal Agarose: peQ LAB, Erlangen

Phosphate Buffered Saline: Sigma-Aldrich

Protein Block Serum-free: Dako®

Puregene Core Kit A, QIAGEN (Lot No. 8272970; Mat No. 1042601), Hilden

QIAmp® DNA Mini Kit (50): QIAGEN, Hilden

RNase A 100mg/mL: QIAGEN

ROTINA35 R: Hettich Zentrifugen, Tübingen

Seramum Grün®chip, O-Dianstaine substrate Solution; Seramum Blau®, TMB/ Substrate Solution: Seramum Diagnostik GmbH Heidensee

Shaker-3012: GFL®, Burgwedel

SmartSpec™3000: BIO-RAD

SNAP i.d.® apparatus, Millipore

SSC buffer 20 x (3 M sodium chloride, 0.3 M sodium citrate, pH = 7.0)

Syringe 5 mL, 0.4 µm filtre, Braun

Thermo Stat plus Shaker: eppendorf, Hamburg

Tris-(2-chloroethyl) amine (CAS- No. 555-77-1)

Tris/ Acetic Acid/ EDTA Buffer 50 x: Bio-Rad Laboratories GmbH, Munich

Tween 20: Sigma

# 4

# Experimental Methods

# 4 Experimental Methods

**Chemicals.** 2-Chloroethyl ethyl sulfide was purchased from TNO (Rijswijk, The Netherlands) with a purity of > 99 % as determined by nuclear magnetic resonance spectroscopy) and Seramun Grün® and Seramun Blau® from Seramun Diagnostica (Heidesee, Germany). All other chemicals were purchased as reagent grade from Sigma-Aldrich (Deisenhofen, Germany) and used without further purification, unless stated otherwise [84].

**Cell Cultures.** HaCaT cells were kindly provided as a donation by Prof. Dr. N. Fusenig of the German Cancer Research Center (Heidelberg, Germany). HaCaT cells are a spontaneously transformed human keratinocyte cell line [85,86]. Standard cell culture flasks (25 $cm^2$, Falcon, Heidelberg, Germany) and the Dulbecco's Modified Eagle Medium/Ham's F12 (DMEM/F12) were used to culture the cells. The DMEM medium was supplemented with 10% fetal calf serum (Life Technologies, Eggenstein, Germany) and glutamine (2.45 mmol/L). The cell cultures were kept at a temperature of 37 °C in a humidified atmosphere with 5% $CO_2$. The time until the cells doubled in number was 22 h. The cells were seeded with $10^5$ cells/$cm^2$. All experiments were performed on the first day after seeding $10^5$ cells/$cm^2$ into new cell cultures flasks (25 $cm^2$, Falcon, Heidelberg, Germany) [84].

**Exposure Protocol.** SM and all other employed SM derivatives were first dissolved in ethanol. The stock solutions containing SM, CEES, and nitrogen mustards were freshly prepared by dilution with Modified Eagle's Medium (MEM) and immediately used after dilution to minimize hydrolysis. The ethanol concentration in the prepared exposure fluids was kept below 1% and control cultures were exposed to solutions containing the same ethanol concentration. HaCaT cells were carefully washed with PBS buffer prior to exposure and incubated at a temperature of 25 °C with the MEM solutions containing different concentrations of either SM (0.1–100 µM; 60 min), CEES (0.3–300 µM; 60 min), or the nitrogen mustards (HN-1, HN-2, or HN-3; 0.3–300 µM; 120 min). After exposure for the indicated time, the cells were carefully washed with PBS. The exposure experiments were performed three times and each immunoslotblot consists of three replicate experiments ($n$ = 9) [84].

**Cell Isolation.** For cell isolation, samples were exposed to 2 mL of 0.05 %-trypsin-EDTA (GIBCO® Invitrogen, Thermo Fisher Scientific, Karlsruhe, Germany). The cells were kept at a temperature of 37 °C throughout the process of trypsinization. Following trypsinization, cell samples were diluted with 13 mL of a DMEM solution containing FKS and transferred to 50 mL tubes. From each of the tubes a volume of 100 µL of the samples was subjected to a cell count (CASY Modell TTC, Innovatis Systems, Reutlingen, Germany). The solutions containing the samples were then

centrifuged for 5 min at 1350 × g (ROTINA35 R, Hettich Zentrifugen, Tübingen, Germany) and the supernatant was removed. The remaining cell pellets were re-suspended in DMEM and the concentration was adjusted to ca. 5–10 · $10^6$ cells/mL. An aliquot of every sample (200 µL) was transferred to a sample tube (1.5 mL) and centrifuged for (5 s, 16.1 × g, Centrifuge 5415 R, Eppendorf, Hamburg, Germany). Following removal of the supernatant medium, the remaining cell pellet in the sample tubes were vortexed [84].

**DNA Isolation.** To isolate DNA samples from the HaCaT cells, the Puregene Core Kit A (QIAGEN, Hilden, Germany) was used. After adding the cell lysis solution (300 µL) to the different cell samples, the mixtures were vortexed for 10 s. To this mixture, 1.5 µL of RNase A (50 mg/mL) was added and samples were incubated for 15 min at a temperature of 37 °C, followed by cooling of the samples to a temperature of 0 °C for 1 min. To the mixture the protein precipitation solution (100 µL) was added, samples were vortexed for 20 s, and a centrifugation at 16.1 × g for 5 min was carried out. The supernatant of each tube was isolated by decantation into isopropanol (300 µL). The isopropanol mixture was carefully mixed by mild shaking and afterwards again centrifuged for 5 min at 16.1 × g. The supernatant was removed and ethanol (300 µL, 70%) was added to the formed pellet. The mixture was centrifuged again for 5 min at 16.1 × g. After removal of the supernatant, samples were dried at room temperature for 15 min. After addition of DNA hydration solution (50 µL), samples were incubated for 1 h at a temperature of 65 °C and mixing of the samples was carried out on a shaker (2/4 digital, IKA® MTS, Staufen, Germany) overnight at moderate speed. To determine the DNA concentration, 1 µL of each sample was used to analyze with a NanoDrop® (Thermo Fisher Scientific, Karlsruhe, Germany). All measurements were carried out at wavelengths of 280 and 260 nm [84].

**DNA Denaturation.** Formamide (8.2 mL) and formaldehyde (0.2 mL) were added to 11.6 mL 50 × Tris/acetic acid/EDTA buffer (Bio-Rad Laboratories GmbH, Munich, Germany) to prepare the DNA-denaturation-buffer-solution. This buffer solution was added to each DNA sample to adjust to a DNA concentration of 50 µg/mL. The samples were incubated at a temperature of 52 °C for 20 min, cooled to 0 °C for 1 min, and held at –80 °C until each sample was frozen. Prior to use, samples were defrosted at room temperature [84].

**Immunoslotblot Technique.** A blotting apparatus (Blotting Unit SHM-48, Harvard Apparatus, U.K.) was used and equipped with a nitrocellulose membrane (Nitrocellulose Transfer Membrane: Protran BA 79, Pore size 0.1 µm; Whatman, Dassel, Germany) and blotting paper. PBS buffer was added to samples of the denaturized DNA to dilute to a concentration of 5 µg/mL. For blotting, 200 µL of each sample were pipetted into a slot.

The DNA samples were blotted onto the membrane with a vacuum of 350 mbar. Afterwards, each slot was washed with PBS (300 µL) and the membrane was air-dried for 15 min. To fixate the DNA onto the membrane, samples were kept at a temperature of 80 °C for 2 h. The membrane was washed twice with a 1:100 SSC buffer (20 × concentrate (3 M sodium chloride, 0.3 M sodium citrate, pH = 7.0) on a shaker at room temperature for a duration of 15 min at moderate speed. Following the washing procedure, the membrane was incubated with a protein block (protein block serum-free, Dako, Hamburg, Germany) for 20 min [84].

**Incubation with the 2F8 Antibody.** An incubation solution was prepared by diluting the 2F8 antibody (2F8 Antibody purified Ab 246, 1.05 mg/mL, BBI, Dundee, Ireland) with antibody diluent (Dako, Hamburg, Germany) to a concentration of 50.25 ng/mL. The membrane was incubated in this solution under continuous tilting over night at a temperature of 4 °C. Following incubation, the membrane was washed four times for 15 min with a PBS solution with 0.1% Tween 20 (Sigma-Aldrich) at room temperature on a shaker. The process was followed by incubation with the HRP-Link (Dako, Hamburg, Germany) solution for 30 min, washing (four times for 10 min) with the same PBS solution, incubation for 30 min with the HRP-Enzyme Dako® ADVANCE™ (Dako, Hamburg, Germany), and washing (four times for 10 min) with the same PBS solution. For each test series, exposed DNA was processed as mentioned above and then dyed. The membranes were dyed by exposure to the following solutions: 3,3'-diaminobenzidin (DAB), SeramunGrün®, or SeramunBlau®. For 3,3'-diaminobenzidin (DAB) the stock solution (50 µL) was added to DAB, filtered (0.4 µm pore size), and added to the membrane. For SeramunGrün® and SeramunBlau® the stock solutions (5 mL) were added to the membrane. Following dyeing, the membranes were washed three times for 10 min with distilled water and dried in ambient conditions [84].

**Analysis of the Membrane.** An Image Scanner III (GE Healthcare; LabScan™ 6.0 Powered by Melanie™, Swiss Institute of Bioinformatics, Switzerland) was used. The settings for the analysis of all membranes were a resolution of 150 bp with the blue filter for the SeramunGrün® or SeramunBlau® dyed samples, while those that were dyed with DAB were analyzed in the reflective mode. The reflective documents mat was removed from the transparency unit during the scanning process. Scanned images were transformed into a Tif file format using the Image J program (version 1.42, Wayne Rasband, NIH, United States) and saved as a negative. The images were analyzed densitometrically with AndorIQ 1.9.1 (Bioimaging, UK). The gray values of each pixel were summed and the background was subtracted. The resulting value was divided by the area of measurement ($mm^2$). The slots on the images and an area of the background with as little dyeing as possible were marked with a fixed rectangle (set ex-ante and used for the analysis of all scanned membranes). The results are given in arbitrary units [84].

**Data Analysis.** The determined data were analyzed with the Mann-Whitney-U-Test (PASW Statistics Version 18) for a statistical evaluation. The results for each concentration and dyeing agent were compared to the negative control (C). The value for the statistical significance $p$ was determined with $p < 0.05$ and $p > 0.05$. This was considered to indicate a statistically significant difference between the exposed sample and C ($p < 0.05$), and a statistically insignificant difference between the exposed sample and C ($p > 0.05$) [84].

**Annotations Concerning the Methods.** The dyeing procedure and the detection of DNA alterations was complicated by the fact that overexposure with the dyeing agent led to a partial dying of the DNA of unexposed HaCAT cells as a false positive. To nonetheless allow for a densitometric analysis of the slot blots, an area of minimal colorization was marked and defined as background. The color intensity of the different slots was then determined relative to the subtracted background from an ex-ante defined rectangle that was used to mark the slots.

The corresponding analysis with the AndorIQ program furnished relative color intensity values for the analyzed slots and the data analysis was then performed using the Mann-Whitney-U-Test for non-parametrical data by SPSS. This test compared the data from each concentration and dyeing agent to the data obtained from the negative control. In this way, statistically significant differences between DNA samples from exposed cells and the ones from the negative control were determined. The rationale for using the Mann-Whitney-U-Test was the assumption that a Gaussian normal distribution could not be justified, even less so with only 9 observations (three membranes with 3 slot blots per concentration per dyeing agent).

The analyzed data were visualized by box plots. Each box plot is constructed in such a way, that it visualizes the maximum and minimum as the upper and lower end of the whiskers attached to the box. The box visualizes the interquartile range containing 50% of the data bordering to the first quartile and the fourth quartile, respectively. In each box plot, the median is visualized by the blue horizontal bar inside each box. The circles indicate outliers.

# 5

# Results

# 5 Results

## 5.1 Detection of DNA Adducts by 2-Chlorethyl Ethyl Sulfide

The HaCAT cells were grown in cell culture flasks according to protocol and exposed for the duration of one hour to the SM derivative CEES in increasing concentrations between 0.3 µM and 300 µM. Altogether, there were eight cell culture bottles, seven were exposed and one was left unexposed as a negative control. After isolation of the DNA and blotting, DAB, Seramun Blau®, as well as Seramun Grün® were investigated as dyeing agents for the visualization of the DNA adducts. In order to obtain statistically relevant data three independent experimental cycles were performed with each dyeing agent and the corresponding membranes were scanned for a subsequent densitometrical analysis. As discernible from the corresponding membrane scans (Figure 10), the initially employed concentrations (0.1–100 µM) were too low for a reliable detection of the slot blots through dyeing. It was therefore decided to shift the concentration range to higher concentrations throughout (0.3–300 µM).


**Figure 10.** Scan of a membrane with the slot blot showing the DNA of HaCAT cells exposed to 2-chlorethyl ethyl sulfide (CEES) and dyed with 3,3'-diaminobenzidin (DAB). From left to right the image shows the DNA expressed from HaCAT cells exposed to an increasing concentration of CEES from the negative control (left, 0 µM) to 100 µM (right).

### 5.1.1 Analysis with 3,3'-Diaminobenzidin Dye

The experiments were repeated independently three times. For the visualization of the DNA adducts caused by CEES the dyeing agent 3,3'-diaminobenzidin (DAB) was used in three cycles. The scan of the corresponding membranes showed that the intensity of the dyed regions increased with an increasing concentration of CEES (Figure 11a), thus indicating a higher number of DNA adducts. All slots and a background area of the scanned membranes were marked and subsequently analyzed densitometrically. The observed dyeing intensities for all analyzed slots per concentration and dyeing agent are given in arbitrary units (a.u.) and the results of the exposed DNA slots were compared with the ones of the negative control using the Mann-Whitney-U-Test (Figure 11b).

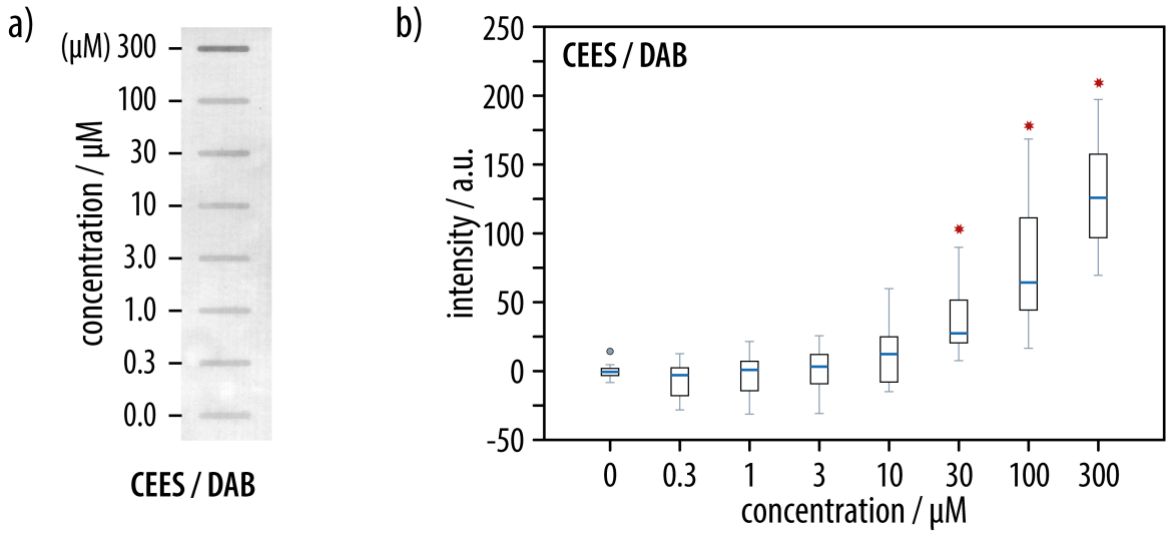


**Figure 11.** **a)** Scan of the membrane with the slot blot showing the DNA of HaCAT cells exposed to 2-chlorethyl ethyl sulfide (CEES) and dyed with 3,3'-diaminobenzidin (DAB). From bottom to top the image shows the DNA expressed from HaCAT cells exposed to an increasing concentration of CEES from the negative control (0 µM) at the bottom to 300 µM at the top of the membrane. **b)** Statistical results of the slot blots of the CEES series dyed with DAB. The x-axis shows the concentration of CEES (given in µM) as well as the negative control. The y-axis shows the intensity (given in a.u.) of the densitometrically analyzed slot blots. The median is included within the box plots (depicted as a blue bar inside the box). Concentrations at which a statistically relevant difference between the exposed sample and the negative control could be detected are marked (✷) and outliers are marked (●).

**Table 3.** Shown below are the calculated data from the analysis of the DNA exposed to CEES and dyed with DAB with the minima, medians, and maxima from the measurements of the DNA slot blots given in arbitrary units (a.u.).

| Concentration of CEES (µM) | Minimum (a.u.) | Median (a.u.) | Maximum (a.u.) |
|---|---|---|---|
| 0 | –8.36 | –0.62 | 14.30 |
| 0.3 | –28.17 | –2.95 | 12.56 |
| 1.0 | –31.29 | 0.87 | 21.48 |
| 3.0 | –30.86 | 3.19 | 25.67 |
| 10.0 | –15.00 | 12.29 | 59.87 |
| 30.0 | 7.49 | 27.42 | 89.94 |
| 100.0 | 16.55 | 64.35 | 168.58 |
| 300.0 | 69.56 | 125.86 | 197.16 |

The analysis showed a significant difference between the slot of the negative control and the different CEES concentrations down to 30 µM on a 5 % level ($p < 0.05$). In other words, this points to a statistically significant difference between the negative control and the exposed DNA for concentrations of CEES equal to or larger than 30 µM. Below concentrations of 30 µM, no statistically significant difference ($p < 0.05$) between the exposed samples of DNA and the

negative control was observed. Accordingly, the employed test does not allow to differentiate between cells, and by extension, human tissue exposed to CEES at concentrations below 30 µM (the detailed results are given in Figure 11 and Table 3). The analysis also demonstrates that the dyeing intensity is not normally distributed, because the median as indicated by the blue bar is not located in the center of the range and the box, respectively (Figure 11b). Both, the median values as well as the interquartile range are increasing in value, which reflects the increasing intensity of dyeing of the slots in line with the increasing concentrations of CEES.

### 5.1.2 Analysis with Seramun Blau® Dye

The visualization of the DNA adducts caused by CEES was explored with the dyeing agent Seramun Blau® in three cycles. The scan of the corresponding membranes showed that the intensity of the dyed regions increased with an increasing concentration of CEES (Figure 12a), thus indicating a higher number of DNA adducts. The corresponding membranes were scanned and all slots plus a background area were marked and analyzed densitometrically. The intensities observed for the exposed DNA slots were compared with the negative control using the Mann-Whitney-U-Test. The analysis showed a significant difference between the blot of the negative control and the different CEES concentrations down to 3 µM (Figure 12b), as indicated by $p < 0.05$. This points to a statistically significant difference between the negative control and the exposed DNA equal to or larger than 3 µM.

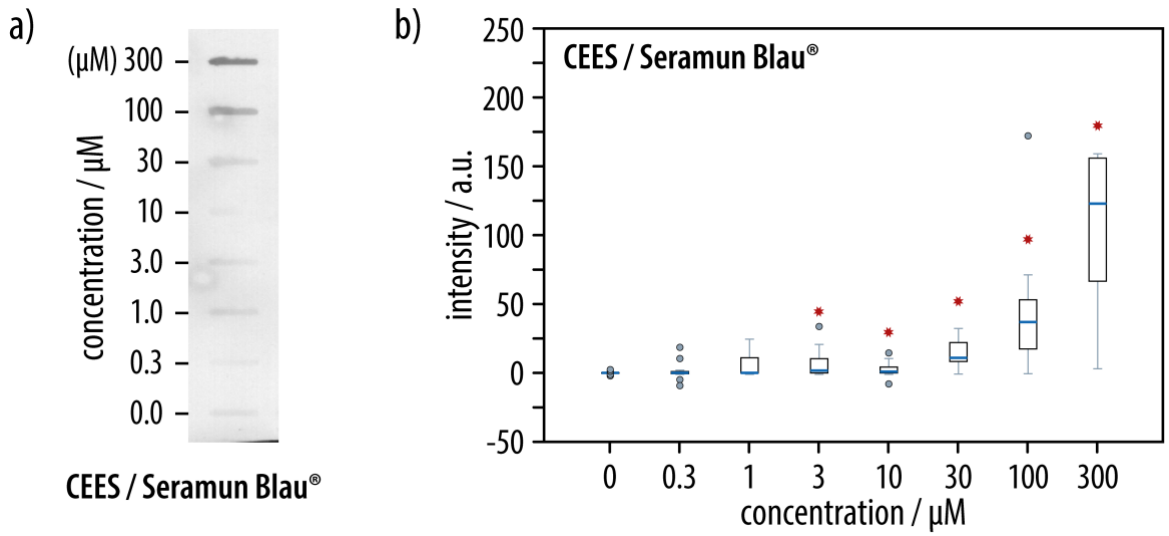


**Figure 12. a)** Scan of the membrane of the blot showing the DNA of HaCAT cells exposed to CEES and dyed with Seramun Blau®. From top to bottom the image shows the DNA expressed from HaCAT cells exposed to a decreasing concentration of CEES with 300 µM at the top of the membrane and the negative control (0 µM) at the bottom. **b)** Statistical results of the CEES series, dyed with Seramun Blau®. The x-axis shows the concentration of CEES (given in µM) as well as the negative control. The y-axis shows the intensity (given in a.u.) determined by densitometric analysis. A statistically significant difference between the negative control and DNA exposed to CEES in this experimental series is shown down to a concentration of 3 µM. Concentrations at which a statistically relevant difference between the exposed sample and the negative control could be detected are marked (✷) and outliers are marked (●).

Concentrations below 3 µM of CEES show no statistically significant difference between the exposed samples and the negative control indicated by *p* exceeding 0.05, suggesting 3 µM as the limit of detection to differentiate for exposure to CEES with Seramun Blau® dyeing. As discernible from the box plot (Figure 12b), the dyeing intensity is not normally distributed. Both, the median values as well as the interquartile range are increasing, which reflects the increasing much higher dyeing intensity for slots with an increased concentration of CEES. For higher concentrations, it is clearly possible to identify the difference compared to the negative control, while the difference becomes less prominent with decreasing concentrations, even though a statically relevant evaluation remains possible.

**Table 4.** Shown below are the analytical data from the analysis of the DNA exposed to CEES and dyed with Seramun Blau®. Tabulated are the minima, medians, and maxima from the measurements of the intensities of the DNA slot blots given in arbitrary units (a.u.).

| Concentration of CEES (µM) | Minimum (a.u.) | Median (a.u.) | Maximum (a.u.) |
|---|---|---|---|
| 0 | –2.13 | –0.01 | 2.4 |
| 0.3 | –9.23 | –0.01 | 18.6 |
| 1.0 | –1.07 | 0.03 | 24.5 |
| 3.0 | –1.07 | 1.69 | 33.7 |
| 10.0 | –7.99 | 0.90 | 14.5 |
| 30.0 | –0.83 | 10.99 | 32.2 |
| 100.0 | –0.54 | 36.98 | 172.1 |
| 300.0 | 3.03 | 122.86 | 159.1 |

### 5.1.3 Analysis with Seramun Grün® Dye

Seramun Grün® was used as a dyeing solution to visualize the DNA adducts caused as a result of exposure of HaCAT cells to CEES at concentrations between 0.3 µM and 300 µM. The depicted membrane shows that a higher dyeing intensity was observed in parallel to the increasing concentration of CEES (Figure 13a), indicating an increasing number of DNA adducts. For Seramun Grün® dyeing, the statistical analysis showed a significant difference between the slot blots of DNA exposed to CEES and the negative control down to a concentration of 30 µM with a value of *p* smaller than 0.05 (Figure 13b).

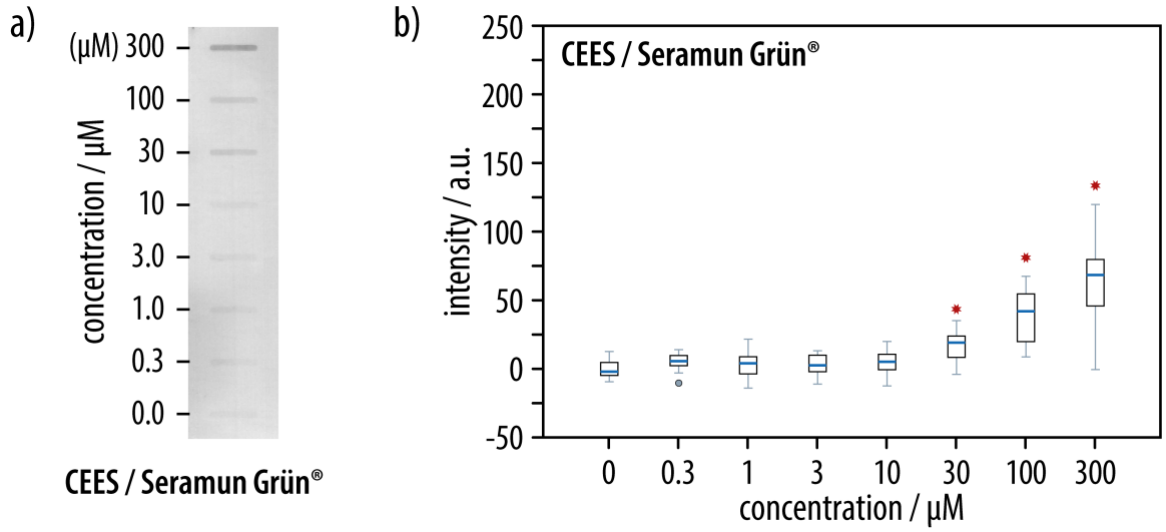


**Figure 13. a)** Scan of the membrane of the blot showing the DNA of HaCAT cells exposed to CEES and dyed with the agent Seramun Grün®. From top to bottom, the image shows the slots with DNA expressed from the HaCAT cells after exposure to a decreasing amount of CEES, with 300 µM at the top and the negative control (0 µM) at the bottom. **b)** Statistical results of the slot blots of the CEES series, dyed with Seramun Grün®. The x-axis shows the concentration of CEES (given in µM) as well as the negative control. The y-axis shows the intensity (given in a.u.) of the densitometrically analyzed slot blots. The median is included within the box plots (depicted as a blue bar). Concentrations at which a statistically significant difference between the negative control and samples exposed to CEES could be detected are marked (✱) and outliers are marked (●).

The interquartile ranges and the medians were also determined and are depicted in the box plot by the box and the blue bar, respectively. For concentrations of CEES smaller than 30 µM no statistically significant difference to the negative control was observed, with values of *p* larger than 0.05. Thus, the Seramun Grün® staining agent allows for the detection of CEES exposure through analysis of DNA samples down to a limit of detection of 30 µM.

**Table 5.** Shown below are the analytical data from the analysis of the DNA exposed to CEES and dyed with Seramun Grün®. The data shown in the table are the minima, medians, and maxima from the measurements of the intensities of the DNA slot blots given in arbitrary units (a.u.).

| Concentration of CEES (µM) | Minimum (a.u.) | Median (a.u.) | Maximum (a.u.) |
|---|---|---|---|
| 0 | –9.34 | –2.05 | 12.66 |
| 0.3 | –10.36 | 5.60 | 13.96 |
| 1.0 | –13.97 | 3.98 | 21.69 |
| 3.0 | –11.04 | 2.57 | 13.25 |
| 10.0 | –12.42 | 5.17 | 19.91 |
| 30.0 | –4.00 | 19.07 | 35.18 |
| 100.0 | 8.75 | 41.90 | 67.44 |
| 300.0 | –0.52 | 68.35 | 119.74 |

## 5.2 Detection of DNA Adducts by Bis(2-Chloroethyl) Sulfide

The HaCAT cells were grown in cell culture flasks according to protocol and exposed to bis(2-chloroethyl) sulfide (SM) for one hour in increasing concentrations in the range from 0.1 µM to 100 µM. Altogether, of the eight cell culture bottles, seven were exposed and one was left unexposed as a negative control. After isolation of the DNA and blotting, DAB as well as Seramun Grün® were investigated as dyeing agents for the visualization of the DNA adducts. Thus, initial tests with DAB suggested that this dyeing agent works very well for SM and the additional investigations with Seramun Grün® were carried out to obtain a data set for comparison. In order to obtain an appropriate statistical assessment three independent experimental cycles were performed with each dyeing agent and the corresponding membranes were scanned for densitometrical analysis.

### 5.2.1 Analysis with 3,3'-Diaminobenzidin Dye

After exposing the HaCAT cells to SM for one hour, the DNA was isolated from the cells and processed in order to blot it onto the membrane forming slots. These slots were then dyed with DAB. An increasing color intensity of the dyed slots could be seen that went in parallel to the increasing concentration of SM (Figure 14a).

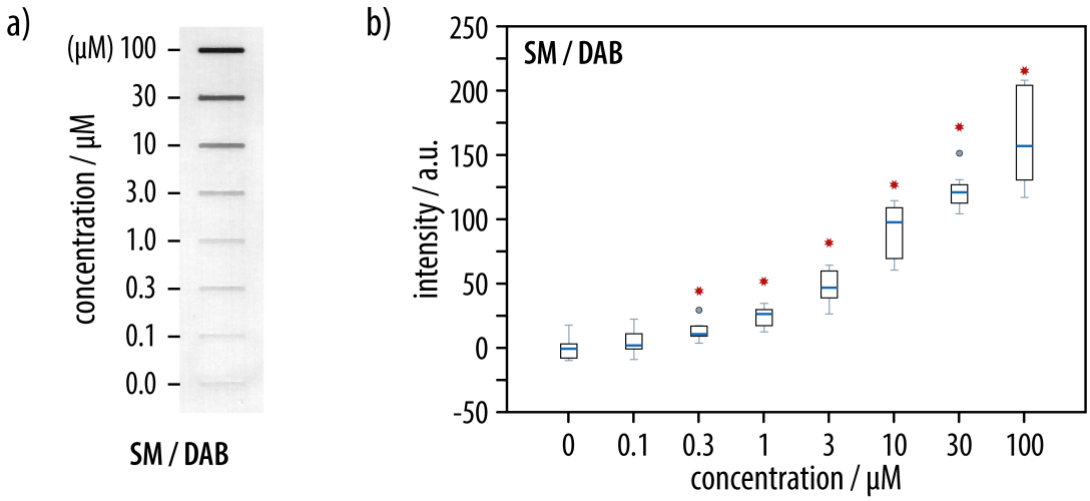


**Figure 14.** **a)** Scan of the membrane of the blot showing the DNA of HaCAT cells exposed to SM and dyed with 3,3'-diaminobenzidin dye (DAB). From top to bottom, the image shows the DNA expressed from the HaCAT cells and exposed to SM with 100µM at the top of the membrane and the negative control (0 µM) at the bottom. **b)** Statistical results of the slot blots of the SM series, dyed with DAB. The x-axis shows the concentration of SM (given in µM) as well as the negative control. The y-axis shows the intensity (given in a.u.) of the densitometrically analyzed slot blots. The median is included within the box plots (depicted as a blue bar). Concentrations at which a statistically relevant difference between the exposed sample and the negative control could be detected are marked (✱) and outliers are marked (●).

The DNA slots were analyzed as described (*vide supra*) and the results were given in arbitrary units and visualized graphically via box plots (Figure 14b). The statistical tests showed significant differences between the exposed samples and the negative control down to a concentration of 0.3 µM SM ($p < 0.05$). Hence, it is possible to detect DNA adducts caused by SM down to 0.3 µM SM., while no significant difference between the negative control and the exposed samples was observed for lower SM concentrations.

**Table 6.** Shown below are the analytical data from the analysis of the DNA exposed to SM and dyed with DAB. The data shown in the table are the minima, medians, and maxima from the measurements of the intensities of the DNA slot blots given in arbitrary units (a.u.).

| Concentration of SM (µM) | Minimum (a.u.) | Median (a.u.) | Maximum (a.u.) |
|---|---|---|---|
| 0 | –9.79 | –0.66 | 17.69 |
| 0.1 | –9.01 | 1.93 | 22.34 |
| 0.3 | 3.62 | 10.73 | 29.34 |
| 1.0 | 12.41 | 26.27 | 34.61 |
| 3.0 | 26.39 | 46.77 | 64.28 |
| 10.0 | 60.52 | 97.67 | 114.47 |
| 30.0 | 104.24 | 120.97 | 151.32 |
| 100.0 | 116.95 | 156.93 | 208.11 |

### 5.2.2 Analysis with Seramun Grün® Dye

During this experimental cycle with Seramun Grün® as a dyeing agent an increasing intensity of dyeing was again observed with increasing concentrations of SM (Figure 15a). The corresponding box plots suggest that a critical difference can be seen down to a concentration of 1.0 µM of SM, with a value of *p* smaller than 0.05 (Figure 15b). This indicates that for SM concentrations below 1.0 µM it is not possible to distinguish between DNA exposed and unexposed to SM, using this method. Comparing the results from the Seramun Grün® dyes and the ones from DAB demonstrates that the limit for detecting DNA adducts caused by SM is lower when using DAB dyeing (concentration of SM lower than 1.0 µM with *p* larger than 0.05 in Seramun Grün® dyeing versus lower than 0.3 µM of SM with *p* larger than 0.05 in DAB). Thus, DAB appears to be more suitable for the detection of DNA adducts caused by SM.

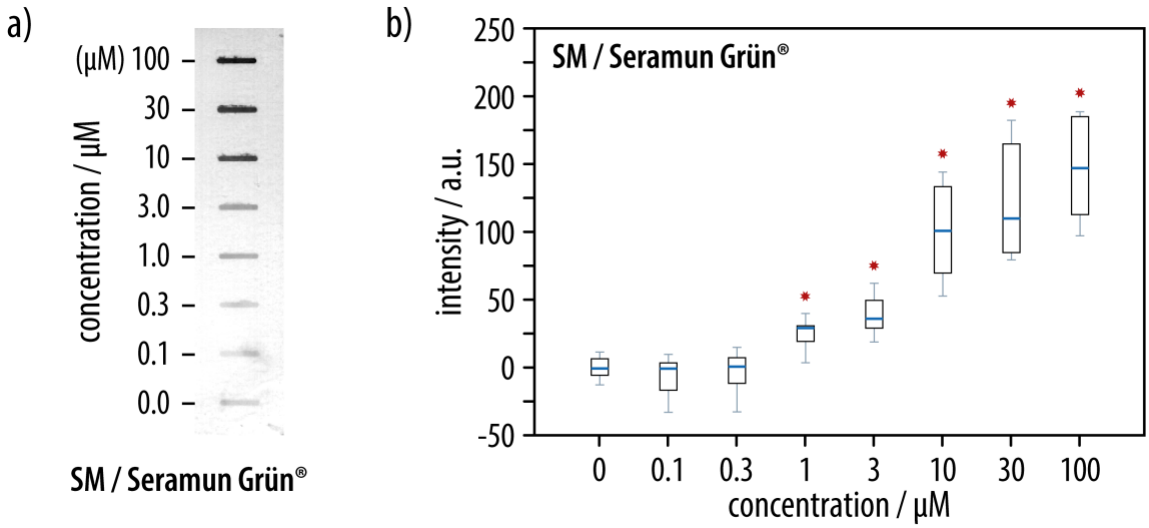


**Figure 15. a)** Scan of the membrane of the blot showing the DNA of HaCAT cells exposed to SM and dyed with the agent Seramun Grün®. From top to bottom the image shows the slot blots of the DNA expressed from the HaCAT cells exposed to a decreasing amount of SM from 100µM at the top of the membrane and the negative control (0 µM) at the bottom. **b)** Statistical results of the slot blots of the SM series, dyed with Seramun Grün®. The x-axis shows the concentration of SM (given in µM) in increasing order as well as the negative control. The y-axis shows the intensity (given in a.u.) of the densitometrically analyzed slot blots. The median is included within the box plots (depicted as a blue bar inside the box). Concentrations at which a statistically relevant difference between the exposed sample and the negative control could be detected are marked (✶) and outliers are marked (●).

**Table 7.** Shown below are the analytical data from the analysis of the DNA exposed to SM and dyed with Seramun Grün®. The data shown in the table are the minima, medians, and maxima from the measurements of the intensities of the DNA slot blots given in arbitrary units (a.u.).

| Concentration of SM (µM) | Minimum (a.u.) | Median (a.u.) | Maximum (a.u.) |
|---|---|---|---|
| 0 | –12.84 | –0.74 | 11.40 |
| 0.1 | –33.04 | –0.79 | 9.67 |
| 0.3 | –32.73 | 0.61 | 14.86 |
| 1.0 | 3.48 | 29.12 | 39.86 |
| 3.0 | 52.62 | 100.70 | 144.16 |
| 10.0 | 97.09 | 146.98 | 188.49 |
| 30.0 | 18.83 | 35.98 | 62.07 |
| 100.0 | 79.31 | 109.80 | 182.22 |

## 5.3 Detection of DNA Adducts by Nitrogen Mustards

To investigate the detection of DNA adducts that are caused by nitrogen mustards, HaCAT cells were grown in cell culture bottles and exposed to the nitrogen mustard (HN) derivatives HN-1, HN-2, or HN-3. Initially the cells were exposed to these HN derivatives for one hour, just as had

been the case in the investigations with SM and CEES. However, realizing that detecting the DNA adducts was very difficult after exposure for 1 h, it was decided to change the time of exposure to two hours while simultaneously raising the concentration range of the HN-derivatives from 0.1–100 µM to 0.3–300 µM. As mentioned above, initially only DAB was used for dyeing, but dyeing the slots of DNA was difficult, and other agents (Seramun Grün® and Seramun Blau®) were tested as well. In order to allow an appropriate statistical assessment three independent experimental cycles were performed for each combination of dyeing agent and nitrogen mustard, the corresponding membranes were scanned, and subjected to densitometrical analysis.

### 5.3.1 Detection of DNA Adducts by Bis(2-Chloroethyl) Ethylamine (HN-1)

#### 5.3.1.1 Analysis with 3,3'-Diaminobenzidin Dye

After exposure of cells to HN-1, densitometric analysis was performed on the corresponding slot blots for the detection of DNA adducts with DAB as dyeing agent. However, the obtained results indicated significant differences between the samples and the negative control ($p < 0.05$) (Figure 16). This can be explained by the median of the negative control, which was larger than most other medians obtained for exposed DNA samples. The negative control actually showed more intense dyeing than the slot blots of the exposed DNA samples, which lead to a false positive significance with $p$ smaller than 0.05 for some of the slots of exposed DNA.

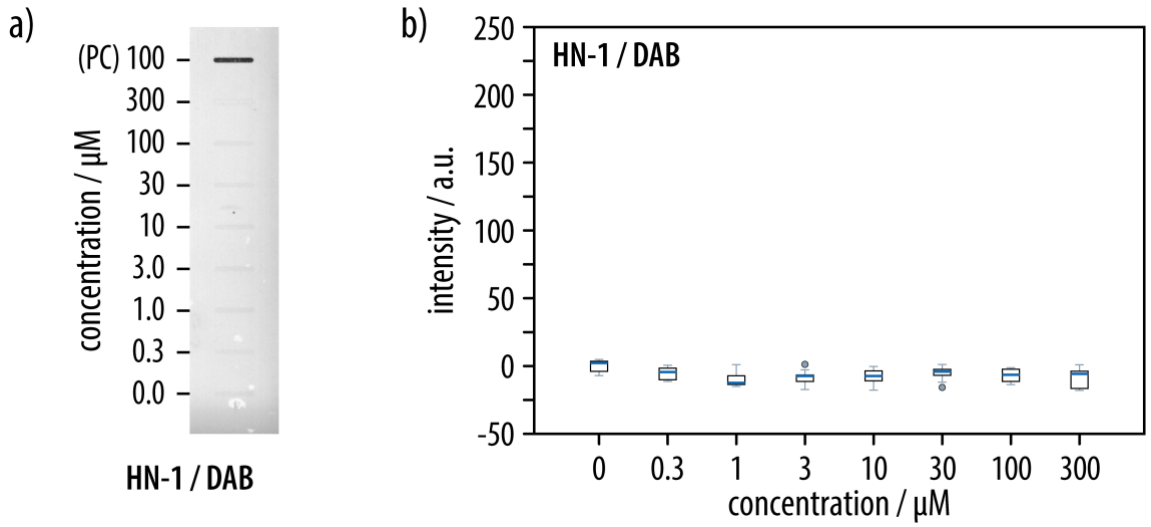


**Figure 16. a)** Scan of the membrane of the blot showing the DNA of HaCAT cells exposed to HN-1 and dyed with the agent DAB. The slot blot of the positive control (PC; DNA exposed to 100 µM of SM) is at the top of the scan. Below the positive control are the slots showing the DNA expressed from the HaCAT cells exposed to a decreasing amount of HN-1 between 300µM and the negative control (0 µM) at the bottom of the membrane. **b)** Statistical results of the slot blots of the HN-1 series, dyed with DAB. The x-axis shows the concentration of HN-1 (given in µM) as well as the negative control. The y-axis shows the intensity (given in a.u.) of the densitometrically analyzed slot blots. The median is included within the box plots (depicted as a blue bar inside the box). There is no statistically relevant difference between the exposed sample and the negative control. Outliers are marked ( ).

**Table 8.** Shown below are the analytical data from the analysis of the DNA exposed to HN-1 and dyed with DAB. The data shown in the table are the minima, medians, and maxima from the measurements of the intensities of the DNA slot blots given in arbitrary units (a.u.).

| Concentration of HN-1 (µM) | Minimum (a.u.) | Median (a.u.) | Maximum (a.u.) |
|---|---|---|---|
| 0 | –7.06 | 2.21 | 4.85 |
| 0.3 | –11.32 | –4.45 | 0.53 |
| 1.0 | –15.06 | –12.43 | 1.08 |
| 3.0 | –17.27 | –7.34 | 1.25 |
| 10.0 | –17.71 | –7.34 | –0.33 |
| 30.0 | –15.75 | –4.10 | 1.09 |
| 100.0 | –13.65 | –6.40 | –1.21 |
| 300.0 | –17.98 | –5.81 | 0.92 |

### 5.3.1.2 Analysis with Seramun Blau® Dye

No significant difference between the negative control and the exposed samples of DNA ($p > 0.05$) was observed when using the Seramun Blau® dye on the HN-1 slot blots (Figure 17). This indicates that it is not possible to differentiate between DNA exposed or unexposed to HN-1. Accordingly, possible DNA adducts induced by exposure of cells to HN-1 can't be recognized.

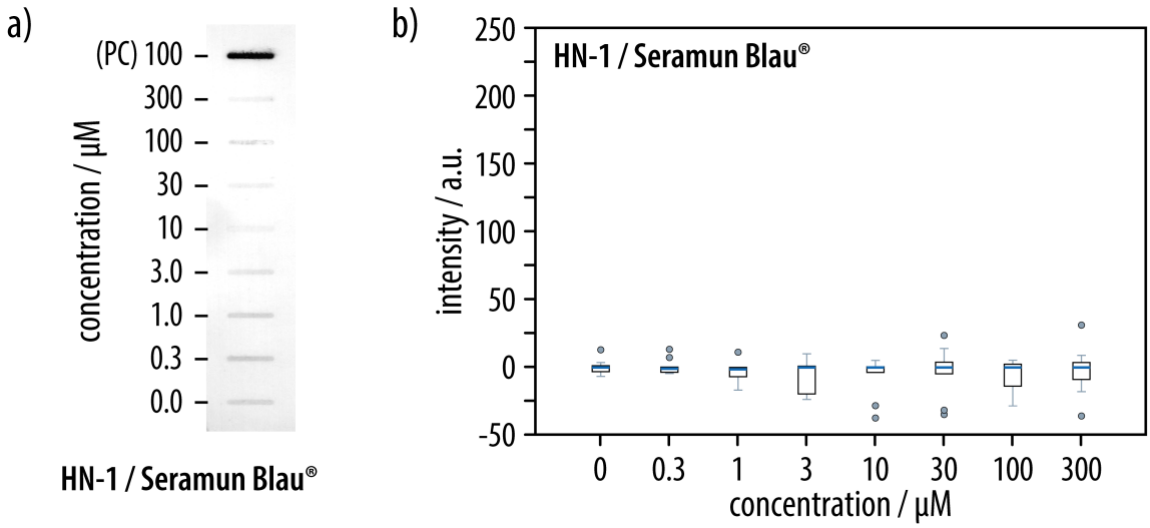


**Figure 17. a)** Scan of the membrane of the blot showing the DNA of HaCAT cells exposed to HN-1 and dyed with the agent Seramun Blau®. The slot blot of the positive control (PC; DNA exposed to 100 µM of SM) is at the top of the scan, followed by the slots that were exposed to decreasing amounts of HN-1 from 300µM to the negative control (0 µM) at the bottom of the membrane. **b)** Statistical results of the HN-1 series, dyed with Seramun Blau®. The x-axis shows the concentration of HN-1 (given in µM) as well as the negative control. The y-axis shows the intensity (given in a.u.) of the densitometrically analyzed slot blots. The median is included in the box plots (depicted as a blue bar inside the box). There is no statistically significant difference between exposed samples and the control. Outliers are marked (●).

**Table 9.** Shown below are the analytical data from the analysis of the DNA exposed to HN-1 and dyed with Seramun Blau®. The data shown in the table are the minima, medians, and maxima from the measurements of the intensities of the DNA slot blots given in arbitrary units.

| Concentration of HN-1 (µM) | Minimum (a.u.) | Median (a.u.) | Maximum (a.u.) |
|---|---|---|---|
| 0 | –7.00 | –0.42 | 12.56 |
| 0.3 | –4.93 | –1.34 | 12.92 |
| 1.0 | –17.13 | –1.77 | 10.80 |
| 3.0 | –24.02 | –0.42 | 9.58 |
| 10.0 | –37.73 | –0.42 | 4.79 |
| 30.0 | –35.15 | –0.42 | 23.17 |
| 100.0 | –28.80 | –0.42 | 4.85 |
| 300.0 | –36.23 | –0.42 | 30.77 |

### 5.3.1.3 Analysis with Seramun Grün® Dye

Using Seramun Grün® for dyeing, the DNA slot blots on the membrane showed a false significant difference between the negative control and the exposed samples with values of $p$ smaller than 0.05 ($p < 0.05$) (Figure 18), analogous to what was seen with DAB.

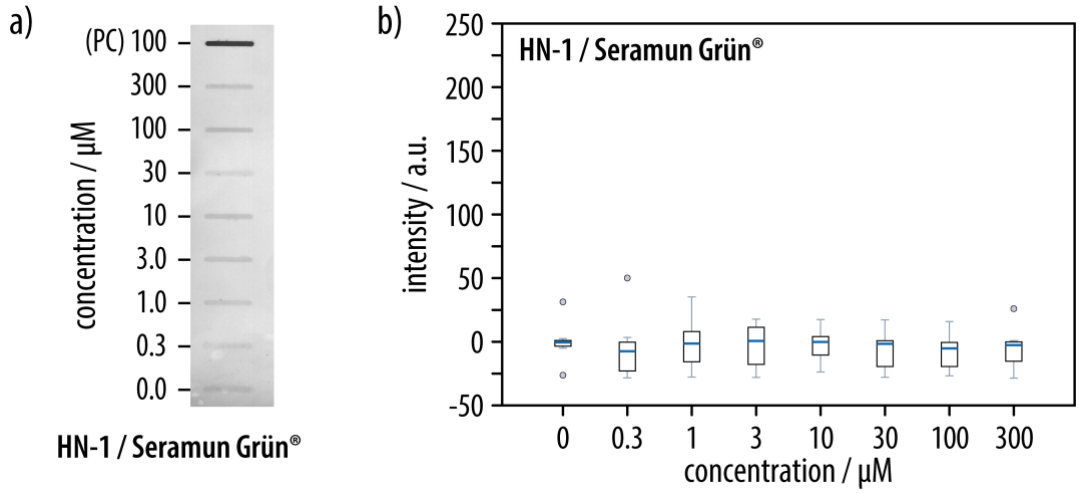


**Figure 18. a)** Scan of the membrane of the blot showing the DNA of HaCAT cells exposed to HN-1 and dyed with the agent Seramun Grün®. The slot blot of the positive control (PC; DNA exposed to 100 µM of SM) is at the top of the scan and followed by slots that were exposed to a decreasing amount of HN-1 between 300µM and the negative control (0 µM) at the bottom of the membrane. **b)** Statistical results of the slot blots of the HN-1 series, dyed with Seramun Grün®. The x-axis shows the concentration of HN-1 (given in µM) as well as the negative control. The y-axis shows the intensity (given in a.u.) of the densitometrically analyzed slot blots. The median is included within the box plots (depicted as a blue bar inside the box). No statistically relevant difference between the exposed sample and the negative control could be detected. Outliers are marked (●).

This can be explained by looking at the dyed membrane, which showed more intense dyeing of the negative control compared to the slots of exposed DNA samples. And after analyzing the median of the negative control, it appears that it is larger than most medians of the exposed DNA samples. This indicates that it is not possible to differentiate between DNA samples, which were exposed to and samples which were not exposed to HN-1.

**Table 10.** Shown below are the analytical data from the analysis of the DNA exposed to HN-1 and dyed with Seramun Grün®. The data shown in the table are the minima, medians, and maxima from the measurements of the intensities of the DNA slot blots given in arbitrary units.

| Concentration of HN-1 (µM) | Minimum (a.u.) | Median (a.u.) | Maximum (a.u.) |
|---|---|---|---|
| 0 | –26.23 | –0.52 | 31.31 |
| 0.3 | –28.30 | –7.46 | 50.07 |
| 1.0 | –27.71 | –1.41 | 35.21 |
| 3.0 | –27.93 | 0.66 | 17.83 |
| 10.0 | –23.73 | –0.17 | 17.48 |
| 30.0 | –27.87 | –1.62 | 17.19 |
| 100.0 | –26.72 | –5.23 | 15.93 |
| 300.0 | –28.53 | –2.63 | 26.00 |

### 5.3.2 Detection of DNA Adducts by Bis(2-Chloroethyl) Methylamine (HN-2)

In analogy to the characterization of samples that were exposed to HN-1, densitometric analysis was performed for the detection of DNA adducts caused by HN-2. Due to the observed general difficulty in detecting DNA adducts caused by HN-2 with the primary monoclonal antibody 2F8, the tests were limited to only DAB and Seramun Grün® as dyeing agents in these experiments.

#### 5.3.2.1 Analysis with 3,3'-Diaminobenzidin Dye

When using DAB for dyeing the DNA after exposure of cells to HN-2, no statistically significant difference between the exposed slot blots and the ones from the negative control were observed ($p > 0.05$; Figure 19). This indicates that DNA exposed to HN-2 cannot be differentiated from unexposed DNA.

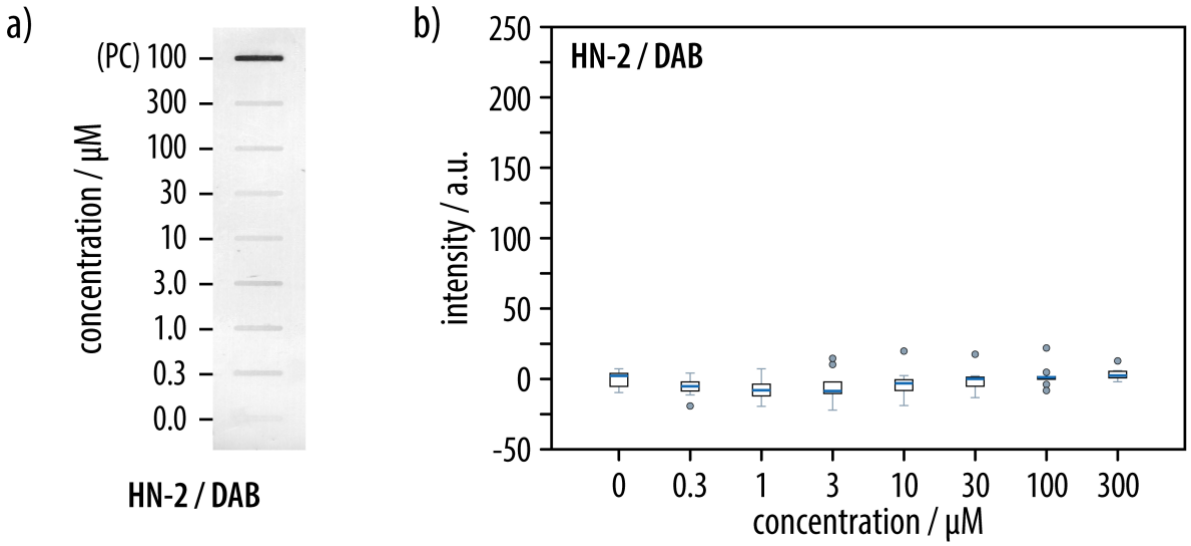


**Figure 19. a)** Scan of the membrane of the blot showing the DNA of HaCAT cells exposed to HN-2 after dyeing with DAB. The slot blot of the positive control (PC; DNA exposed to 100 µM of SM) is at the top of the scan followed by the slots exposed to a decreasing amount of HN-2 between 300µM and the negative control (0 µM) at the bottom of the membrane. **b)** Statistical results of the slot blots of the HN-2 series, dyed with DAB. The x-axis shows the concentration of HN-2 (given in µM) in increasing order as well as the negative control. The y-axis shows the intensity (given in a.u.) as determined by densitometric analysis. The median is included within the box plots (depicted as a blue bar inside the box). No statistically relevant difference between the exposed sample and the negative control could be detected. Outliers are marked ( ).

**Table 11.** Shown below are the analytical data from the analysis of the DNA exposed to HN-2 and dyed with DAB. The data shown in the table are the minima, medians, and maxima from the measurements of the intensities given in arbitrary units (a.u.) of the DNA slot blots.

| Concentration of HN-2 (µM) | Minimum (a.u.) | Median (a.u.) | Maximum (a.u.) |
|---|---|---|---|
| 0 | –9.63 | 2.22 | 7.23 |
| 0.3 | –19.16 | –5.20 | 4.18 |
| 1.0 | –19.39 | –7.96 | 7.26 |
| 3.0 | –22.10 | –8.58 | 14.62 |
| 10.0 | –18.86 | –3.07 | 19.80 |
| 30.0 | –13.28 | 0.05 | 17.54 |
| 100.0 | –8.21 | 1.23 | 21.99 |
| 300.0 | –2.01 | 2.39 | 12.81 |

### 5.3.2.2 Analysis with Seramun Grün® Dye

After cells were exposed to HN-2 and the DNA was extracted, the agent Seramun Grün® was used to dye the DNA blots on the membrane (Figure 20a). The statistical analysis of the densitometric

data shows no *p* smaller than 0.05. This indicates that no difference between the negative control and a DNA sample exposed to HN-2 was detected and that DNA exposed to HN-2 cannot be differentiated from unexposed DNA.

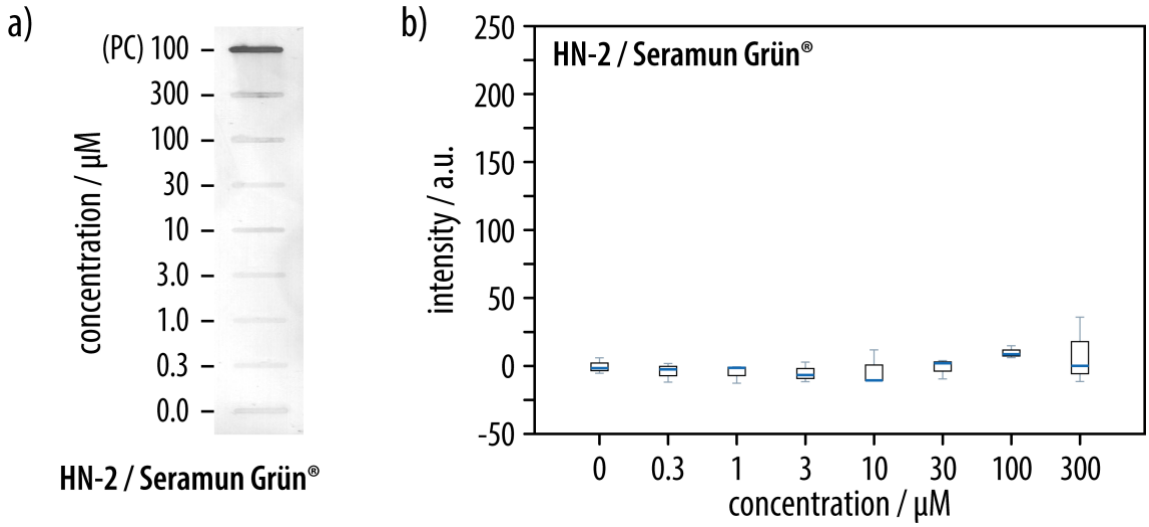


**Figure 20. a)** Scan of the membrane of the blot showing the DNA of HaCAT cells exposed to HN-2 and dyed with the agent Seramun Grün®. The slot blot of the positive control (PC; DNA exposed to 100 µM of SM) at the top of the scan is followed by slots exposed to decreasing amounts of HN-2 between 300µM and the negative control (0 µM) at the bottom of the membrane. **b)** Statistical results of the slot blots of the HN-2 series, dyed with Seramun Grün®. The x-axis shows the concentration of HN-2 (given in µM) in increasing order as well as the negative control. The y-axis shows the intensity (given in a.u.) as determined by densitometric analysis. The median is included within the box plots (depicted as a blue bar within the box). No statistically relevant difference between the exposed sample and the negative control was detected. Outliers are marked (●).

**Table 12.** Shown below are the analytical data from the analysis of the DNA exposed to HN-2 and dyed with Seramun Grün®. The data shown in the table are the minima, medians, and maxima from the measurements of the intensities of the DNA slot blots given in arbitrary units (a.u.).

| Concentration of HN-2 (µM) | Minimum (a.u.) | Median (a.u.) | Maximum (a.u.) |
|---|---|---|---|
| 0 | –5.07 | –5.07 | 6.33 |
| 0.3 | –11.56 | –11.56 | 2.12 |
| 1.0 | –12.39 | –12.39 | –0.33 |
| 3.0 | –11.28 | –11.28 | 3.16 |
| 10.0 | –10.46 | –10.46 | 12.18 |
| 30.0 | –9.24 | –9.24 | 4.25 |
| 100.0 | 6.47 | 6.47 | 15.17 |
| 300.0 | –11.17 | –11.17 | 36.19 |

### 5.3.3 Detection of DNA Adducts by Tris(2-Chloroethyl) Amine (HN-3)

The DNA exposed to HN-3 was processed, blotted onto a membrane, incubated with the primary antibody 2F8, the HRP link, and the HRP enzyme. Then the blotted DNA was exposed to a dyeing agent (DAB or Seramun Grün®). After realizing, that 2F8 was again not suitable for detecting the DNA adducts, we tried to detect DNA alterations caused by HN-derivatives by increasing the concentration of the primary antibody 2F8. As discussed in more detail below, however, this did not resolve the encountered issues.

#### 5.3.3.1 Analysis with 3,3'-Diaminobenzidin Dye

After densitometric analysis of the membrane and statistical evaluation of the data, no significant difference between the box plot of the negative control and the DNA slots of the different concentrations of HN-3 were detected (Figure 21). This was demonstrated by looking at the results of the Mann-Whitney-U-Test with $p > 0.05$. Values of $p > 0.05$ indicate a statistically insignificant difference between the DNA of the negative control and the exposed one.

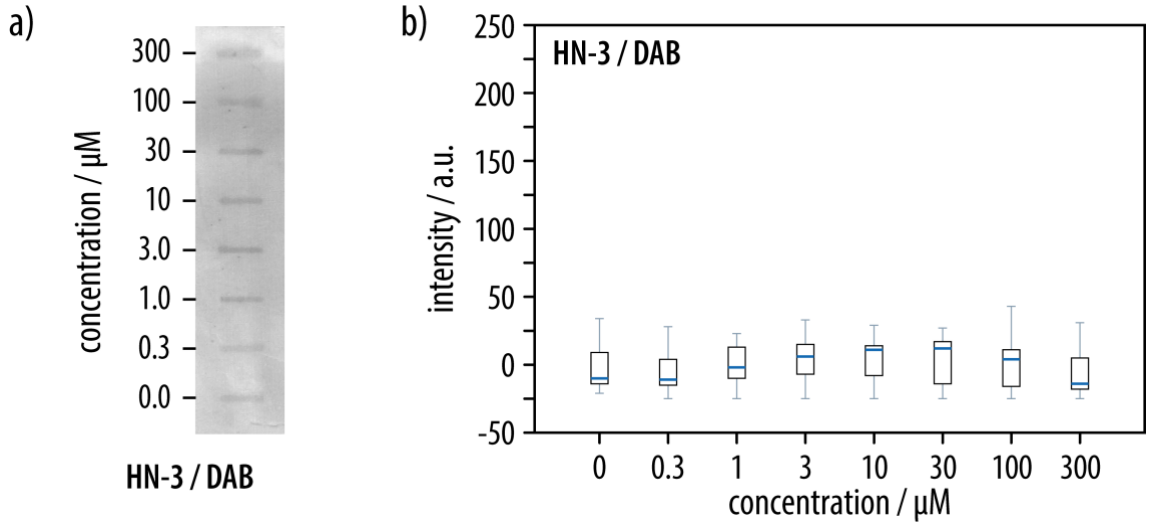


**Figure 21. a)** Scan of the membrane of the blot showing the DNA of HaCAT cells exposed to HN-3 and dyed with DAB. The image shows the DNA expressed from HaCAT cells exposed to a decreasing amount of HN-3 with 300µM at the top of the membrane and ends with the negative control (0 µM) at the bottom. **b)** Statistical results of the slot blots of the HN-3 series, dyed with DAB. The x-axis shows the concentration of HN-3 (given in µM) as well as the negative control. The y-axis shows the intensity (given in a.u.) of the densitometrically analyzed slot blots. The median is included within the box plots (depicted as a blue bar inside the box). No statistically relevant difference between the exposed sample and the negative control could be detected.

**Table 13.** Shown below are the analytical data from the analysis of the DNA exposed to HN-3 and dyed with DAB. The data shown in the table are the minima, medians, and maxima from the measurements of the intensities of the DNA slot blots given in arbitrary units.

| Concentration of HN-3 (µM) | Minimum (a.u.) | Median (a.u.) | Maximum (a.u.) |
|---|---|---|---|
| 0 | –21.00 | –10.00 | 34.00 |
| 0.3 | –25.00 | –2.00 | 23.00 |
| 1.0 | –25.00 | –11.00 | 28.00 |
| 3.0 | –25.00 | 6.00 | 33.00 |
| 10.0 | –25.00 | 11.00 | 29.00 |
| 30.0 | –25.00 | 12.00 | 27.00 |
| 100.0 | –25.00 | 4.00 | 43.00 |
| 300.0 | –25.00 | –14.00 | 31.00 |

### 5.3.3.2 Analysis with Seramun Grün® Dye

After the standard procedure of cell treatment, the DNA exposed to HN-3 was isolated, processed, and blotted. Then the membrane was incubated with the primary antibody 2F8, the HRP-Enzyme, HRP-Link, and dyed with Seramun Grün® (Figure 22).

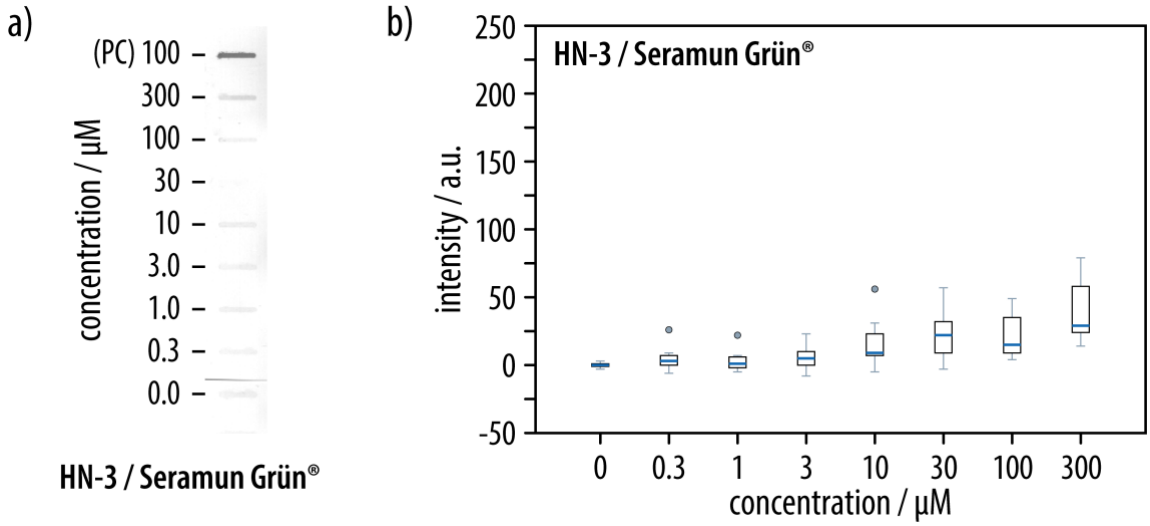


**Figure 22. a)** Scan of the membrane of the blot showing the DNA of HaCAT cells exposed to HN-3 and dyed with the agent Seramun Grün®. The image shows the DNA expressed from HaCAT cells. The slot blot of the positive control (PC; DNA exposed to 100 µM of SM) is at the top of the scan. DNA expressed from the HaCAT cells exposed to a decreasing amount of HN-3 with 300µM below the positive control and the negative control (0 µM) at the bottom. **b)** Statistical results of the slot blots of the HN-3 series, dyed with Seramun Grün®. The x-axis shows the concentration of HN-3 (given in µM) in increasing order as well as the negative control. The y-axis shows the intensity (given in a.u.) of the densitometrically analyzed slot blots. The median is included within the box plots (depicted as a blue bar inside the box). No statistically relevant difference between the exposed sample and the negative control could be detected. Outliers are marked (●).

The statistical results are depicted in box plots. The intensity increases in parallel to the concentration, with an increasing median (blue bar within the box) and an interquartile range (IQR) moving towards higher signal intensities. This can be explained by an increasing number of DNA adducts in parallel to an increasing concentration of HN-3, which results in a more intense dyeing. But when comparing these data to the graphs of the other HN-3 experiments as well as the graphs of the other HN-derivatives, the results of this HN-3 Seramun Grün® dye analysis should rather be interpreted as coincidence.

**Table 14.** Shown below are the analytical data from the analysis of the DNA exposed to HN-3 and dyed with Seramun Grün®. The data shown in the table are the minima, medians, and maxima from the measurements of the intensities of the DNA slot blots given in arbitrary units.

| Concentration of HN-3 (µM) | Minimum (a.u.) | Median (a.u.) | Maximum (a.u.) |
|---|---|---|---|
| 0 | –3.00 | 0.00 | 3.00 |
| 0.3 | –5.00 | 1.00 | 22.00 |
| 1.0 | –6.00 | 3.00 | 26.00 |
| 3.0 | –8.00 | 5.00 | 23.00 |
| 10.0 | –5.00 | 9.00 | 56.00 |
| 30.0 | –3.00 | 22.00 | 57.00 |
| 100.0 | 4.00 | 15.00 | 49.00 |
| 300.0 | 14.00 | 29.00 | 79.00 |

#### 5.3.3.3 Double Concentration of 2F8-Antibody with 3,3'-Diaminobenzidin Dye

To facilitate the detection of DNA adducts formed after exposure to nitrogen mustards, additional experiments were carried out with HN-3, following the standard procedure, but with double the concentration of the 2F8 antibody that binds to DNA adducts. The corresponding slot blot was subjected to densitometric analysis and the statistical results are depicted in box plots (Figure 23). The analysis shows values of $p > 0.05$, indicating no statistically significant difference between the negative control and the DNA samples exposed to HN-3.

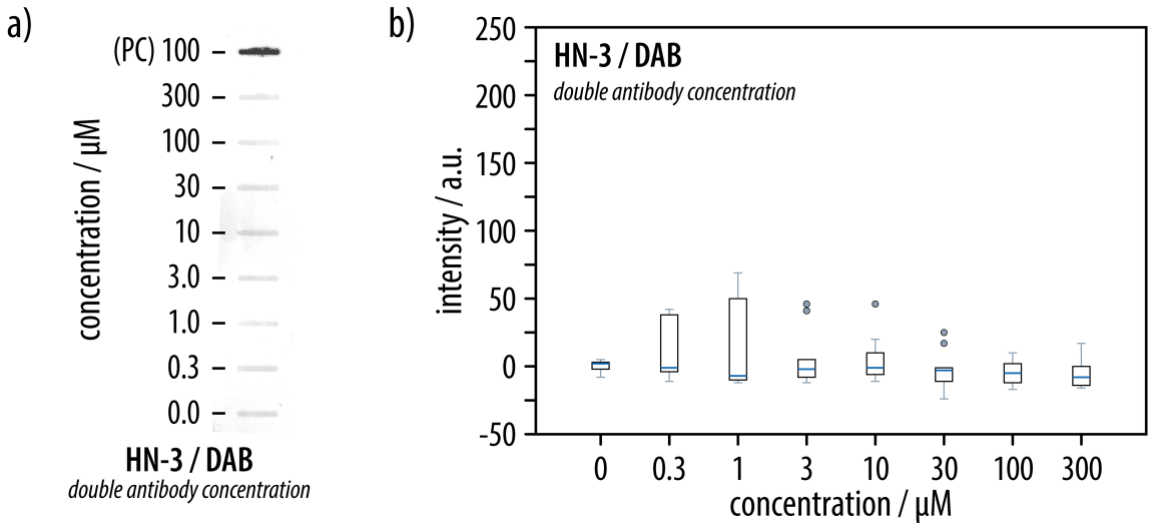


**Figure 23. a)** Scan of the membrane of the blot showing the DNA of HaCAT cells exposed to HN-3 and dyed with the agent DAB and with double the concentration of the primary antibody 2F8. The image shows the DNA expressed from HaCAT cells. The slot blot of the positive control (PC; DNA exposed to 100 µM of SM) is at the top of the scan. The DNA expressed from the HaCAT cells exposed to a decreasing amount of HN-3 with 300µM below the positive control and the negative control (0 µM) at the bottom of the membrane. **b)** Statistical results of the slot blots of the HN-3 series, dyed with DAB and double the concentration of the primary antibody 2F8. The x-axis shows the concentration of HN-3 (given in µM) as well as the negative control. The y-axis shows the intensity (given in a.u.) of the densitometrically analyzed slot blots. The median is included within the box plots (depicted as a blue bar within the box). No statistically relevant difference between the exposed sample and the negative control could be detected. Outliers are marked ( ).

**Table 15.** Shown below are the analytical data from the analysis of the DNA exposed to HN-3, incubated to double the concentration of the primary antibody 2F8, and dyed with DAB. The data shown in the table are the minima, medians, and maxima from the measurements of the intensities of the DNA slot blots given in arbitrary units.

| Concentration of HN-3 (µM) | Minimum (a.u.) | Median (a.u.) | Maximum (a.u.) |
|---|---|---|---|
| 0 | –8.00 | 2.00 | 5.00 |
| 0.3 | –12.00 | –7.00 | 69.00 |
| 1.0 | –11.00 | –1.00 | 42.00 |
| 3.0 | –12.00 | –2.00 | 46.00 |
| 10.0 | –11.00 | –1.00 | 46.00 |
| 30.0 | –24.00 | –3.00 | 25.00 |
| 100.0 | –17.00 | –5.00 | 5.00 |
| 300.0 | –16.00 | –8.00 | 69.00 |

## 5.4 Attempt at an Improved Visualization of DNA Samples

The ultimate goal of the herein described investigations is the development of a field test that may allow for a detection of the exposure to SM and its different derivatives. A major drawback of the

methodology that was employed in the laboratory was the length of the process of the visualization of the DNA samples. In order to further accelerate this process, an attempt for improving the procedure was performed by employing the SNAP i.d.® apparatus for the incubation steps. The use of the apparatus allows for a fast and homogenous distribution of applied reagents during incubation steps, which could significantly reduce the time of these steps and thereby the time from DNA extraction to detection.

The previously described standard procedure after exposure of cells to SM was applied to prepare the membranes, and the different incubation steps were then performed with the SNAP i.d.® apparatus to test its utility. According to the protocol provided by Millipore, the manufacturer of the SNAP i.d.® apparatus, the concentration of the primary antibody has to be slightly increased in order to achieve comparable results. To check this requirement, a series of additional experiments was carried out in which the concentration of 2F8 as well as the time of exposure were increased stepwise. Staining of the thus prepared membranes was then performed with DAB as a staining agent.

However, throughout these experiments with the changed incubation procedure, the results were not as expected. The outcome with regard to staining of DNA adducts was inferior when compared to that previously obtained via the standard protocol. The details can be readily seen from a comparison of a blot of a membrane that was developed with the SNAP i.d. apparatus and a primary antibody concentration of 1:20.000 for 12 hours with the blot of a membrane that was obtained by the standard protocol (Figure 24). Thus, the experimental protocol using the SNAP i.d. apparatus would need further optimization, e.g., by potentially starting with the time of incubation with the primary antibody.

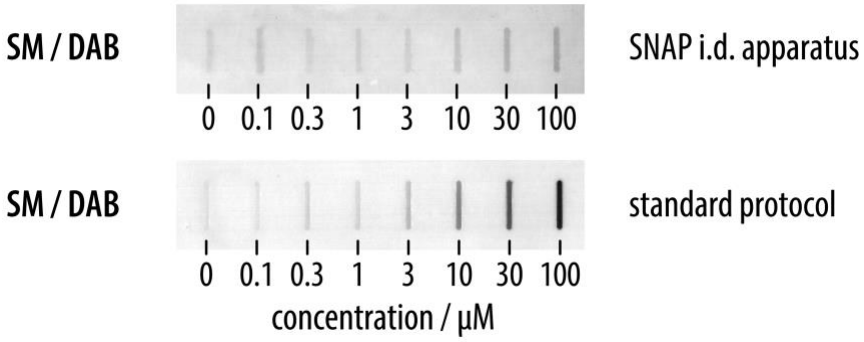


**Figure 24.** Comparison of the scanned DNA slot blots exposed to SM and (top) incubated from the step using the primary antibody 2F8 onwards either with the SNAP i.d. apparatus or (bottom) incubated following the standard protocol described above. Both slot blots were dyed in the last step with the agent DAB.

# Discussion

# 6 Discussion

In this work, we investigated a method for the detection of a specific DNA adduct caused by SM and other alkylating agents, in particulary CEES, HN-1, HN-2, and HN-3. The chosen approach relies on the fact that, after relevant exposure, SM forms DNA adducts at specific binding sites within the DNA. The most predominant adduct is N7-hydroxyethylthioethyl-2´-deoxyguanosine (N7-HETE-dG) [55]. A highly specific monoclonal antibody (2F8) was developed against this N7-guanine adduct.

The 2F8-antibody has been shown to be a useful tool in a toxicokinetic study and in human blood samples of SM victims [87].

As blisters are the most striking effect of SM on skin, the detection level of any skin test should be below the vesicating dose. Skin blisters are characterized by keratinocyte apoptosis in the stratum basale. Keratinocyte apoptosis is induced in vitro at concentrations above 100 µM SM (60 min of exposure) after 24 h. Thus, in our experiments, the period of exposure towards SM was set to one hour with concentrations ranging between 0.1 and 100 µM. Under these conditions, it was possible to visualize the DNA adducts by the means of immunoslotblot with chromogenic dyes and using densitometry for quantification. The advantage of the chromogenic visualization system is the simplicity of use and unnecessary complex imaging systems compared to fluorescent dyes. However, the disadvantage is the inferior signal-to-noise ratio [84] .

Comparing the effects of the two dyeing agents DAB and Seramun Grün® showed that DAB allows for the detection of DNA adducts down to a concentration of 0.3 µM while with Seramun Grün® only a reliable detection of DNA adducts at SM concentration of 1.0 µM or higher was possible. This indicates that DAB is more suited than Seramun Grün® in detecting DNA adducts caused by SM. However, both dyeing agents were able to detect DNA adducts at concentrations of SM clearly below the vesicant threshold, which is above 100 µM of SM [64]. Hence, when selecting one of them to use for dyeing in order to analyze the immunoslot blots densitometrically in a ready-to-use Kit, one has to consider, that Seramun Grün® is easier to handle, while suitable DAB solutions need to be prepared and filtered. If looking at the final goal – developing a rapid and reliable field test – Seramun Grün® is more likely to be useful.

The next alkylating agent we investigated was CEES, because of its properties similar to SM as well as the fact, that it is used as a substitute for tests concerning the detection of, protection against as well as the decontamination of SM [88]. When investigating CEES it was found that DNA adducts caused by CEES was only detected at higher concentrations (30 µM for DAB and Seramun Grün®, 3 µM for Seramun Blau®). In accordance with the chemical structure of CEES showing only one residue, that can bind to the DNA, the requirement for higher concentrations appears quite

logical [25]. These different reactivities are reflected in the corresponding $LD_{50}$ concentrations of SM and CEES in mice ranging between 9.7 mg/kg for percutaneous and 19.3 mg/kg for oral and 1425 mg/kg for percutaneous and 566 mg/kg for oral application, respectively [88]. In conclusion, it appears that the monoclonal antibody 2F8 can detect less adducts, subsequently leading to a less intense dyeing with CEES when compared to the results obtained for the same concentrations of SM.

Whereas the dyeing agents all performed similar on samples exposed to SM, the use of Seramun Blau® allows to detect DNA adducts at lower concentrations of CEES exposure compared to Seramun Grün® or DAB dyeing. However, the reason why Seramun Blau® was able to detect DNA adducts in CEES at a lower concentration than Seramun Grün® and DAB is not clear. It could be a user specific problem.

Nitrogen mustards with military relevance contain two chlorethyl groups similar to SM. Thus, we also investigated the usefulness of the 2F8-antibody to detect adducts of HN-1, -2, and -3 at N7-guanine. Detecting DNA adducts induced by the different HN-derivatives was not possible.

There might be three reasons why no signal of DNA adducts formed by the HN-derivatives were detected. First, no DNA adducts are formed by the HN-derivatives. Second, the adducts are too different from the ones formed by SM and CEES to induce binding by the 2F8 antibody. This could be particularly true, since 2F8 was specifically developed to bind to DNA adducts formed by SM and it is not yet fully understood in what way HN-derivatives alter the DNA. And the third reason could be the fact, that SM in general forms DNA adducts faster than Nitrogen Mustards [7]. The two hours for which the investigated cells were exposed to the different Nitrogen Mustards might not have been sufficient for the formation of enough DNA adducts to allow for their detection. However, we also incubated the cells once for 24 hours with HN-2 and were still unable to detect DNA adducts.

To conclude, the process of detecting DNA adducts caused by the SM derivatives HN-1, HN-2, and HN-3 needs further investigations and a more specific antibody.

In general, the organs that are affected the most after contact to SM are the eyes, the skin, and the lungs. Accordingly, among the best possible tissues for detecting DNA adducts caused by SM and its derivatives would be the skin due to the ease of access, e.g. via skin biopsies from exposed areas. To mimic the reaction of similar cell types to SM and its derivatives, HaCAT cells were employed in a cell culture (human immortalized keratinocytes/cells from the skin) and exposed to SM. It needs to be considered, that the isolation of DNA from a cell culture, as carried out in the context of the present thesis, is much easier and less time consuming than isolating DNA from a skin biopsy.

We had no difficulties in detecting DNA adducts caused by SM. However, to further speed up the process we investigated the usefulness of the SNAP i.d. blotting apparatus. This device is supposed to shorten the time of exposure to the primary antibody as well as the HRP-Link and HRP-Enzyme by skipping the final overnight incubation step with the primary antibody. However, operation according to the standard protocol of the apparatus did not work as the dyeing results obtained after its use did not compare well with the results obtained by the developed standard procedure. Presumably, the exposure protocol with the apparatus needs to be optimized, but was beyond the scope of this thesis.

A more sensitive method for detecting exposure to SM is by detecting alkylated albumin (HETE-CP) via LC-ESI-MS-MS [41]. Recently, during the Syrian war, this method was used to confirm exposure of civilians to SM [11,78]. However, this method required high-tech machinery and is at the moment not compatible for a field test. Therefore, the detection of DNA adducts from skin cells could be much more accessible on site.

A concentration of SM between 100 µM–1mM can cause cell death and 100–300 µM of SM can cause the formation of vesicles or blisters [64]. Comparing the threshold concentration of SM at which a victim can develop blisters and the threshold concentration at which the testing methodology allows for the detection of DNA adducts formed by SM, shows that we are able to detect exposure to SM via the detection of DNA adducts at concentrations at which victims do not even develop blisters. Thus, the threshold concentration for detecting DNA adducts for SM obtained with the employed testing procedure were found to be between 0.3 µM (when using DAB as a dyeing agent) and 1 µM (when using Seramun Grün® as a dyeing agent), and low thresholds were also determined for CEES (3 µM–30 µM).

To conclude, a comparison of the initially defined objectives and the obtained results illustrates that the developed methodology allows for the detection of DNA adducts formed by SM and CEES, but not for those formed by nitrogen mustards. Interestingly, DNA adducts formed by SM and CEES could be detected at concentrations below the threshold dose for forming blisters, which is especially important for further following-up on patients after an actual exposure to vesicant agents. Moreover, a dyeing solution was found that is easy to use and needs no further processing before application to the membrane, which simplifies the methodology and potentially allows for its use in the field. Finally, the results obtained in the context of the present thesis are a promising starting point for the development of a field test, especially if further experiments should show that the use of the SNAP i.d. apparatus in an improved process can expedite the analysis.

# 7

# Outlook

# 7 Outlook

More work needs to be done to develop an adequate and fast method to detect DNA adducts formed by SM and its derivatives. It was already attempted to improve the method by using the SNAP i.d. apparatus to expedite the incubation of the membrane with the primary antibody and the various enzymes, and dyeing solutions. The best concentrations of the primary antibody 2F8 and the enzymes for the use of the SNAP i.d. apparatus need to be determined by titrations. If the process with the SNAP i.d. apparatus yields promising results, the overnight incubation with the 2F8 antibody could be skipped and one experimental cycle would be shortened to a couple of hours or even less.

Next to reducing the duration of the process, the detection from human skin would be desirable to make the test applicable in the setting of a field laboratory.

Alternatively, it would be advantageous to also use the method for blood samples, by employing a different kit to isolate the DNA. Moreover, with an appropriate blood kit, the step in which the DNA needs to be dissolved overnight could also be eliminated. However, a reliable detection at much lower concentrations is required for the use with blood samples.

Adapting the developed method for usage in field laboratories is an important goal. In addition to a facile test that can be used in proximity to areas affected by CWA, it would be desirable to strengthen the test by expanding the insights that are gained from the analysis of DNA adducts. For example, it could be possible to estimate the concentration of SM a victim was exposed to in the limits of a certain range of concentrations, e.g. between 100–300 µM of SM. To achieve this, an external sample with standard DNA that was exposed to a defined concentration of SM could be used for a calibration based on the comparison of the corresponding slots.

To conclude, it is of utmost importance to continue working on this method, especially when considering the most recent developments in Syria and other countries that showcase that CWAs are unfortunately not yet a thing of the past.

# 8

# References

# 8 References


1 Szinicz L, Worek F, Thiermann H, Kehe K, Eckert S, Eyer P. Development of antidotes: problems and strategies. *Toxicology* 2007; **233**: 23–30.

2 United Nations. 2015. http://www.un.org/en/index.html (accessed Dec 2, 2015).

3 Wattana M, Bey T. Mustard gas or sulfur mustard: an old chemical agent as a new terrorist threat. *Prehospital Disaster Med* 2009; **24**: 19-29-31.

4 Young CL, Ash D, Driskell WJ, Boyer AE, Martinez RA, Silks LA, Barr JR. A rapid, sensitive method for the quantitation of specific metabolites of sulfur mustard in human urine using isotope-dilution gas chromatography-tandem mass spectrometry. *J Anal Toxicol* 2004; **28**: 339–345.

5 OPCW. Eliminating Chemical Weapons. OPCW. 2021. https://www.opcw.org/our-work/eliminating-chemical-weapons (accessed Nov 2, 2021).

6 Balali-Mood M, Hefazi M. The pharmacology, toxicology, and medical treatment of sulphur mustard poisoning. *Fundam Clin Pharmacol* 2005; **19**: 297–315.

7 Dacre JC, Goldman M. Toxicology and pharmacology of the chemical warfare agent sulfur mustard. *Pharmacol Rev* 1996; **48**: 289–326.

8 Oppenheimer A. The Threat of Chemical Weapons: Use by Non-State Actors. OPCW. 2008; published online Nov 28. https://www.opcw.org/media-centre/news/2008/11/threat-chemical-weapons-use-non-state-actors (accessed Oct 25, 2018).

9 Steindl D, Boehmerle W, Körner R, Praeger D, Haug M, Nee J, Schreiber A, Scheibe F, Demin K, Jacoby P, Tauber R, Hartwig S, Endres M, Eckhardt KW. Novichok nerve agent poisoning. *The Lancet* 2021; **397**: 249–252.

10 Vale JA, Marrs TC, Maynard RL. Novichok: a murderous nerve agent attack in the UK. *Clin Toxicol* 2018; **56**: 1093–1097.

11 John H, Koller M, Worek F, Thiermann H, Siegert M. Forensic evidence of sulfur mustard exposure in real cases of human poisoning by detection of diverse albumin-derived protein adducts. *Arch Toxicol* 2019; **93**: 1881–1891.

12 John H, van der Schans MJ, Koller M, Spruit HET, Worek F, Thiermann H, Noort D. Fatal sarin poisoning in Syria 2013: forensic verification within an international laboratory network. *Forensic Toxicol* 2018; **36**: 61–71.

13 Weir AGA, Makin S, Breeze J. Nerve agents: emergency preparedness. *BMJ Mil Health* 2020; **166**: 42–46.

14 Ilyushina M, Shukla S, Halasz S. Kremlin critic Alexey Navalny, discharged from hospital after poisoning, must now weigh his next moves. edition.cnn.com. 2020; published online Sept 23. https://edition.cnn.com/2020/09/23/europe/alexey-navalny-hospital-discharge-intl/index.html (accessed Feb 11, 2021).

15 Weibrecht K, Rhyee S, Manuell ME, Longo C, Boyer EW, Brush E. Sulfur mustard exposure presenting to a community emergency department. *Ann Emerg Med* 2012; **59**: 70–74.

16 Everts S. When Chemicals Became Weapons Of War. *Am Chem Soc Chem Eng News* 2015; **93**: 6–21.

17 Sun Y, Ong KY. Detection Technologies for Chemical Warfare Agents and Toxic Vapors. CRC Press, 2004.

18 Ellison DH. Handbook of chemical and biological warfare agents. Boca Raton: CRC Press LLC, 2000.

19 Ellison DH. Emergency Action for Chemical and Biological Warfare Agents. CRC Press, 2000.

20 Goldfrank's toxicologic emergencies, 8th ed. New York: McGraw-Hill, Medical Pub. Division, 2006.

21 Ehl D. Salisbury: What we know a year after the Skripal poison attack. *04 March 2019* https://www.dw.com/en/salisbury-what-we-know-a-year-after-the-skripal-poison-attack/a-47757214 (accessed Aug 19, 2021).

22 James S. Stratagems, Combat, and 'Chemical Warfare' in the Siege Mines of Dura-Europos. *Archaeol Ins* 2011; **Vol. 115**: pp 69-101.

23 Lombard M. The tip cross-sectional areas of poisoned bone arrowheads from southern Africa. *J Archaeol Sci Rep* 2020; **33**: 102477.

24 Kehe K, Szinicz L. Medical aspects of sulphur mustard poisoning. *Toxicology* 2005; **214**: 198–209.

25 Shakarjian MP, Heck DE, Gray JP, Sinko PJ, Gordon MK, Casillas RP, Heindel ND, Gerecke DR, Laskin DL, Laskin DL, Laskin JD. Mechanisms mediating the vesicant actions of sulfur mustard after cutaneous exposure. *Toxicol Sci Off J Soc Toxicol* 2010; **114**: 5–19.

26 Photograph of German infantry men during a gas attack in WW I. Picture dating 1916/1918, photographer unknown. copyright Bundesarchiv (Bild 183-R05923); o. Ang. BArch, Bild 183-R05923 / o. Ang. .

27 Ghabili K, Agutter PS, Ghanei M, Ansarin K, Shoja MM. Mustard gas toxicity: the acute and chronic pathological effects. *J Appl Toxicol JAT* 2010; **30**: 627–643.

28 Braut-Hegghammer M. Red Lines Matter. *Foreign Aff* 2013; published online May 7. http://www.foreignaffairs.com/articles/139369/malfrid-braut-hegghammer/red-lines-matter (accessed Oct 16, 2013).

29 OPCW. Organisation for the Prohibition of Chemical Weapons. 2015. https://www.opcw.org/ (accessed Dec 2, 2015).

30 Gunkel C. Irakischer Giftgasangriff - Geruch von Müll und süssen Äpfeln. *Spiegel* 2013; published online March 15. https://www.spiegel.de/geschichte/giftgasangriff-auf-halabdscha-1988-a-951065.html (accessed Nov 17, 2020).

31 Üzümcü A. United Nations Security Council: Statement by the Director-General OPCW. 2018; published online March 20. https://www.opcw.org/sites/default/files/documents/ODG/uzumcu/United_Nations_Security_Council_Statement_by_the_Director-General_OPCW__Ambassador_Ahmet_Uzumcu.pdf (accessed Oct 26, 2018).

32 Peplow M. What now for the world´s chemical weapons watchdog? *R Soc Chem Chem World Opin* 2018; published online April 13. https://www.chemistryworld.com/opinion/what-now-for-the-worlds-chemical-weapons-watchdog/3008896.article (accessed Nov 17, 2020).

33 Balali-Mood, Mathews, Pita, Rice, Romano, Thiermann, Willems. Practical Guide for Medical Management of Chemical Warfare Casualties. 2019.

34 Bundeszentrale für politische Bildung. Genfer Protokoll zum Verbot chemischer und biologischer Waffen. 2015; published online June 16, 2005. https://www.bpb.de/politik/hintergrund-aktuell/208302/1925-genfer-protokoll).

35 OPCW. Organisation for the Prohibition of Chemical Weapopns Convention of the Developement, Production, Stockpiling and Use of Chemical Weapons and on their Destruction. 2005; published online July 29, 2005.

36 Asseburg M. Beitritt zur Chemiewaffenkonvention – Chance. Kurz Gesagt. 2013; published online Oct 17. https://www.handelsblatt.com/meinung/gastbeitraege/gastbeitrag-syrischer-beitritt-zur-chemiewaffenkonvention-ist-eine-chance/8954492.html?ticket=ST-15202-nOIf93bW3gVNAzdGQ1Y4-cas01.example.org (accessed Nov 17, 2020).

37 Photograph taken during World War I entitled "The blind leading the blind" showing men of the 55th British Division that were casualties of a poison gas attack. Photograph taken on 10 April 1918, photographer unknown. Copyright World History Archive (WHA_013_0030).

38 Black RM. History and perspectives of bioanalytical methods for chemical warfare agent detection. *J Chromatogr B Analyt Technol Biomed Life Sci* 2010; **878**: 1207–1215.

39 OPCW, United Nations - Security Council. Third report of the Organization for the Prohibition of Chemical Weapons-United Nations Joint Investigative Mechanism. United Nations - Security Council; OPCW, 2016.

40 Organisation for the Prohibition of Chemical Weapons (OPWC) Executive Council. Decision: OPCW-United Nations Joint Investigative Mechanism Reports on Chemical Weapons Use in the Syrian Arab Republic. The Hague, 2016.

41 Gandor F, Gawlik M, Thiermann H, John H. Evidence of Sulfur Mustard Exposure in Human Plasma by LC-ESI-MS-MS Detection of the Albumin-Derived Alkylated HETE-CP Dipeptide and Chromatographic Investigation of Its Cis/Trans Isomerism. *J Anal Toxicol* 2015; **39**: 270–279.

42 Lohs K. Synthetische Gifte: zur Chemie, Wirkung und militärischen Bedeutung. Deutscher Militärverlag, 1974.

43 Gilman A. The Biological Actions and Therapeutic Applications of the B-Chloroethyl Amines and Sulfides. *SCIENCE* 1946; **Vol. 103**, No. 2675.

44 Berenblum I, Riley-Smith. The anti-carcinogenic action of dichlorodiethylsulphide (mustard gas). *1931*; **34 (6)**: 731–746.

45 Fox M, Scott D. The genetic toxicology of nitrogen and sulphur mustard. *Mutat Res* 1980; **75**: 131–168.

46 Weinberger B, Laskin JD, Sunil VR, Sinko PJ, Heck DE, Laskin DL. Sulfur mustard-induced pulmonary injury: therapeutic approaches to mitigating toxicity. *Pulm Pharmacol Ther* 2011; **24**: 92–99.

47 Aktories K, Forth W, Allgaier C. Allgemeine und spezielle Pharmakologie und Toxikologie: für Studenten der Medizin, Veterinärmedizin, Pharmazie, Chemie und Biologie sowie für Ärzte, Tierärzte und Apotheker : mit 305 Tabellen. München: Elsevier, Urban & Fischer, 2009.

48 Munro NB, Talmage SS, Griffin GD, Waters LC, Watson AP, King JF, Hauschild V. The sources, fate, and toxicity of chemical warfare agent degradation products. *Environ Health Perspect* 1999; **107**: 933–974.

49 Bundeswehr Institute of Pharmacology and Toxicology. Technical grade of Sulfur Mustard. .

50 National Toxicology Program. NTP 12th Report on Carcinogens. *Rep Carcinog Carcinog Profiles US Dept Health Hum Serv Public Health Serv Natl Toxicol Program* 2011; **12**: 1–499.

51 Kehe K, Thiermann H, Balszuweit F, Eyer F, Steinritz D, Zilker T. Acute effects of sulfur mustard injury--Munich experiences. *Toxicology* 2009; **263**: 3–8.

52 Papirmeister B, Gross CL, Meier HL, Petrali JP, Johnson JB. Molecular basis for mustard-induced vesication. *Fundam Appl Toxicol Off J Soc Toxicol* 1985; **5**: S134–S149.

53 Kehe K, Balszuweit F, Steinritz D, Thiermann H. Molecular toxicology of sulfur mustard-induced cutaneous inflammation and blistering. *Toxicology* 2009; **263**: 12–19.

54 Vijayaraghavan R, Kulkarni A, Pant SC, Kumar P, Rao PVL, Gupta N, Gautam A, Ganesan K. Differential toxicity of sulfur mustard administered through percutaneous, subcutaneous, and oral routes. *Toxicol Appl Pharmacol* 2005; **202**: 180–188.

55 van der Schans GP, Mars-Groenendijk R, de Jong LPA, Benschop HP, Noort D. Standard operating procedure for immunuslotblot assay for analysis of DNA/sulfur mustard adducts in human blood and skin. *J Anal Toxicol* 2004; **28**: 316–319.

56 Andreassen PR. DNA damage responses and their many interactions with the replication fork. *Carcinogenesis* 2005; **27**: 883–892.

57 Wong-Riley M. Energy metabolism of the visual system. *Eye Brain* 2010; 99.

58 Zhang W, Li H, Ogando DG, Li S, Feng M, Price FW, Tennessen JM, Bonanno JA. Glutaminolysis is Essential for Energy Production and Ion Transport in Human Corneal Endothelium. *EBioMedicine* 2017; **16**: 292–301.

59 U.S. Department of Health and Human Services; Public Health Service; Agency for Toxic Substances and Disease Registry. TOXICOLOGICAL PROFILE FOR SULFUR MUSTARD (UPDATE). 2003; published online Sept. 2003.

60 Jugg BJA, Hoard-Fruchey H, Rothwell C, Dillman JF, David J, Jenner J, Sciuto AM. Acute Gene Expression Profile of Lung Tissue Following Sulfur Mustard Inhalation Exposure in Large Anesthetized Swine. *Chem Res Toxicol* 2016; **29**: 1602–1610.

61 The National Academies Press. Acute Exposure Guideline Levels for Selected Airborne Chemicals: Volume 3. 2001. http://www.nap.edu/openbook.php?record_id=10902 (accessed June 29, 2014).

62 Watson A, Opresko D, Young R, Hauschild V. Development and Application of Acute Exposure Guideline Levels (AEGLs) for Chemical Warfare Nerve and Sulfur Mustard Agents. *J Toxicol Environ Health Part B* 2006; **9**: 173–263.

63 Saladi RN, Smith E, Persaud AN. Mustard: a potential agent of chemical warfare and terrorism. *Clin Exp Dermatol* 2006; **31**: 1–5.

64 Simbulan-Rosenthal CM, Ray R, Benton B, Soeda E, Daher A, Anderson D, Smith WJ, Rosenthal DS. Calmodulin mediates sulfur mustard toxicity in human keratinocytes. *Toxicology* 2006; **227**: 21–35.

65 Kadar T, Dachir S, Cohen L, Sahar R, Fishbine E, Cohen M, Turetz J, Gutman H, Buch H, Brandeis R, Horwitz V, Solomon A, Amir A. Ocular injuries following sulfur mustard exposure--pathological mechanism and potential therapy. *Toxicology* 2009; **263**: 59–69.

66 Amini H, Solaymani-Dodaran M, Mousavi B, Alam Beladi SN, Soroush MR, Abolghasemi J, Vahedian-Azimi A, Salesi M, Guest PC, Sahebkar A, Ghanei M. Long-term Health Outcomes Among Survivors Exposed to Sulfur Mustard in Iran. *JAMA Netw Open* 2020; **3**: e2028894.

67 Rowell M, Kehe K, Balszuweit F, Thiermann H. The chronic effects of sulfur mustard exposure. *Toxicology* 2009; **263**: 9–11.

68 Panahi Y, Roshandel D, Sadoughi MM, Ghanei M, Sahebkar A. Sulfur Mustard-Induced Ocular Injuries: Update on Mechanisms and Management. *Curr Pharm Des* 2017; **23**: 1589–1597.

69 International Agency for Research on Cancer. Chemical Agents and Related Occupations; IARC Monographs on the Evaluation of Carcinogenic Risks to Humans; Volume 100 F. 2012. https://publications.iarc.fr/Book-And-Report-Series/Iarc-Monographs-On-The-Identification-Of-Carcinogenic-Hazards-To-Humans/Chemical-Agents-And-Related-Occupations-2012.

70 Schmidt A, Steinritz D, Rothmiller S, Thiermann H, Scherer AM. Effects of sulfur mustard on mesenchymal stem cells. *Toxicol Lett* 2018; **293**: 98–104.

71 Marquardt H, Marquardt-Schäfer-Barth, editors. Toxikologie: mit 378 Tabellen, 3., vollst. überarb. und erw. Aufl. Stuttgart: WVG, Wiss. Verl.-Ges, 2013.

72 Steinritz D, Striepling E, Rudolf K-D, Schröder-Kraft C, Püschel K, Hullard-Pulstinger A, Koller M, Thiermann H, Gandor F, Gawlik M, John H. Medical documentation, bioanalytical evidence of an accidental human exposure to sulfur mustard and general therapy recommendations. *Toxicol Lett* 2016; **244**: 112–120.

73 U.S. Army Medical Research Institute of Chemical Defense, Chemical Casualty Care Division. Medical management of chemical casualties handbook. Mclean, VA: International Medical Publishing, 2000.

74 Veress LA, Hendry-Hofer TB, Loader JE, Rioux JS, Garlick RB, White CW. Tissue Plasminogen Activator Prevents Mortality from Sulfur Mustard Analog–Induced Airway Obstruction. *Am J Respir Cell Mol Biol* 2013; **48**: 439–447.

75 Etemad L, Moshiri M, Balali-Mood M. Advances in treatment of acute sulfur mustard poisoning – a critical review. *Crit Rev Toxicol* 2019; **49**: 191–214.

76 Balszuweit F, Menacher G, Schmidt A, Kehe K, Popp T, Worek F, Thiermann H, Steinritz D. Protective effects of the thiol compounds GSH and NAC against sulfur mustard toxicity in a human keratinocyte cell line. *Toxicol Lett* 2016; **244**: 35–43.

77 Kung AC, Stephens MB, Darling T. Phytophotodermatitis: bulla formation and hyperpigmentation during spring break. *Mil Med* 2009; **174**: 657–661.

78 John H, Siegert M, Gandor F, Gawlik M, Kranawetvogl A, Karaghiosoff K, Thiermann H. Optimized verification method for detection of an albumin-sulfur mustard adduct at Cys34 using a hybrid quadrupole time-of-flight tandem mass spectrometer after direct plasma proteolysis. *Toxicol Lett* 2016; **244**: 103–111.

79 OPCW. NOTE BY THE TECHNICAL SECRETARIAT STATUS OF LABORATORIES DESIGNATED FOR THE ANALYSIS OF AUTHENTIC BIOMEDICAL SAMPLES. 2020; published online Oct 2.

80 OPCW. Executive Council Eighty-Fifth Session. 2017 https://www.opcw.org/sites/default/files/documents/EC/85/en/ec85inf02r1_e_.pdf (accessed Nov 4, 2021).

81 Boyer AE, Ash D, Barr DB, Young CL, Driskell WJ, Whitehead RD Jr, Ospina M, Preston KE, Woolfitt AR, Martinez RA, Silks LAP, Barr JR. Quantitation of the sulfur mustard metabolites 1,1'-sulfonylbis[2-(methylthio)ethane] and thiodiglycol in urine using isotope-dilution Gas chromatography-tandem mass spectrometry. *J Anal Toxicol* 2004; **28**: 327–332.

82 Noort D, Fidder A, Hulst AG, de Jong LP, Benschop HP. Diagnosis and dosimetry of exposure to sulfur mustard: development of a standard operating procedure for mass spectrometric analysis of haemoglobin adducts: exploratory research on albumin and keratin adducts. *J Appl Toxicol JAT* 2000; **20**, Suppl 1: S187-S192.

83 Noort D, Fidder A, Benschop HP, De Jong LPA, Smith JR. Procedure for monitoring exposure to sulfur mustard based on modified edman degradation of globin. *J Anal Toxicol* 2004; **28**: 311–315.

84 Kehe K, Schrettl V, Thiermann H, Steinritz D. Modified immunoslotblot assay to detect hemi and sulfur mustard DNA adducts. *Chem Biol Interact* 2013; **206**: 523–528.

85 Boukamp P, Petrussevska RT, Breitkreutz D, Hornung J, Markham A, Fusenig NE. Normal keratinization in a spontaneously immortalized aneuploid human keratinocyte cell line. *J Cell Biol* 1988; **106**: 761–771.

86 Fusenig NE, Breitkreutz D, Dzarlieva RT, Boukamp P, Bohnert A, Tilgen W. Growth and differentiation characteristics of transformed keratinocytes from mouse and human skin in vitro and in vivo. *J Invest Dermatol* 1983; **81**: 168s–175s.

87 Benschop HP, van der Schans GP, Noort D, Fidder A, Mars-Groenendijk RH, de Jong LPA. Verification of Exposure to Sulfur Mustard in Two Casualties of the Iran-Iraq Conflict. *J Anal Toxicol* 1997; **21**: 249–251.

88 Gautam A, Vijayaraghavan R, Sharma M, Ganesan K. Comparative toxicity studies of sulfur mustard (2,2'-dichloro diethyl sulfide) and monofunctional sulfur mustard (2-chloroethyl ethyl sulfide), administered through various routes in mice. *J Med CBR Def* 2006; **4**: 1–22.

# Appendix

## Publikationsliste

### Publications (peer-reviewed)

"Modified immunoslotblot assay to detect hemi and sulfur mustard DNA adducts." Kehe, K.; Schrettl V.; Thiermann H.; Steinritz, D.; *Chem Biol Interact.* **2013** Dec, *206*, 523–528.

"L-Arginine in the treatment of valproate overdose – five clinical cases." Schrettl, V.; Felgenhauer, N.; Rabe, C.; Fernando, M.; Eyer, F.; *Clin Toxicol (Phila)*. **2017** Apr; 55(4): 260-266.

"Synthetic cathinones in Southern Germany – characteristics of users, substance-patterns, co-ingestions, and complications." Romanek, K.; Stenzel, J.; Schmoll, S.; Schrettl, V.; Geith, S.; Eyer, F.; Rabe, C.; *Clin Toxicol (Phila).* **2017** Jul; 55(6):573-578.

### Poster Presentations

"*A Snake Bite by the Dinniki´s Viper: A Case Report*" Schrettl, V.; Felgenhauer, N.; Eyer, F.; **2015**, poster presentation at the 35th International Congress of the European Association of Poisons Centres and Clinical Toxicologists (EAPCCT); 26–29 May 2015, St. Julian´s, Malta.

"*A case of mono-intoxication with duloxetine: Clinical presentation and serum levels*" Schrettl, V.; Stenzel, J.; Pfab, R.; Eyer, F.; **2016**, poster presentation at the 36th International Congress of the European Association of Poisons Centres and Clinical Toxicologists (EAPCCT); 24–27 May 2016, Madrid.

"*A Case Report: Reversible neurotoxicity, gastrointestinal, and visual disturbances after consumption of the onion earthball: Scleroderma cepa Pers.*" Haberl, B.; Schrettl, V.; Pfab, R.; Eyer, F; **2016**, poster presentation at the Conference of the 36th International Congress of the European Association of Poisons Centres and Clinical Toxicologists (EAPCCT); 24-27 May 2016, Madrid.